

Persistence of a wind-driven fire regime in Mediterranean France over the past 8200 years revealed by a marine paleoecological record

The Holocene
1–16

© The Author(s) 2025



Article reuse guidelines:

sagepub.com/journals-permissions

DOI: 10.1177/09596836251350236

journals.sagepub.com/home/hol



Marion Genet,^{1,2} Anne-Laure Daniau,¹ Florent Mouillot,³
Bérangère Leys,⁴ Maria-Angela Bassetti,² Julien Azuara,⁵ Bassem Jalali,⁶
Marie-Alexandrine Sicre,⁷ Serge Berné² and Muriel Georget¹

Abstract

Data on paleofire activity in southeastern France during the Holocene are still lacking thus limiting our capability to anticipate fire regime shifts under climate change. Here, we present a 8.2 ky-long high-resolution time-series of microscopic charcoal (microcharcoal) particles from a marine sediment core retrieved from the Rhone prodelta, in the Gulf of Lions (NW Mediterranean Sea). Fire frequency, episodes, size and types of burnt vegetation were determined by quantifying microcharcoal and analysing its morphometry. Our results indicate an increase in biomass burning and fire frequency combined with a decrease in the mean elongation ratio from the Northgrippian (8.2–4.2 ka) to the Meghalayan (4.2–0 ka) stage. This pattern is interpreted as reflecting a shift from the burning of graminoids in closed mesophytic forests during the Northgrippian to the burning of shrub communities in open Mediterranean habitats during the Meghalayan. We also identified 20 fire episodes over the past 8.2 ka, occasionally coinciding with human occupations. Large fires occurred during cold events and summer droughts conditions of the Northgrippian. We relate this finding to negative phases of the North Atlantic Oscillation (NAO) and increased fuel load under wet winter conditions and fuel flammability under dry and strong summer winds. Besides climate and vegetation, human activity is likely to be an additional driver of fire during the Meghalayan. Southeastern France is currently identified as a region with a high wind-driven fire risk, although its fire regime analysis is biased by intensive fire suppression. We suggest that wind-driven large fires is an inherent element of fire and weather patterns in this area rather than the result of fire suppression strategies leading to uncontrollable large fires.

Keywords

climate change, cold events, fire, Holocene, marine sediment, microcharcoal

Received 10 April 2025; revised manuscript accepted 1 May 2025

Introduction

Fire plays a crucial role on plant distribution and represents one of the most important terrestrial disturbance on Earth (Bond et al., 2005). Major economic costs are associated with wildfire management, fire damage losses to human assets, ecosystem services and ecological values (Bowman et al., 2009; Chuvieco et al., 2023; Lohman et al., 2007). These costs are expected to rise, in particular across the Mediterranean Region, a European hotspot of fire activity (San-Miguel-Ayanz et al., 2019). The frequency and extent of large wildfires in this region are expected to increase under future climate scenarios (Grünig et al., 2023; Ruffault et al., 2020), further disturbing the ecosystems and human assets. However, uncertainties remain in long-term projections as they are based on contemporary statistical relationships between fire, climate and fuel, neglecting potential change of these interactions due to direct impacts of CO₂ on vegetation composition and distribution or human impacts (Hantson et al., 2016). Furthermore, divergent fire activity is predicted under drier versus wetter climatic conditions in Mediterranean-type ecosystems in relation to precipitation-related variables (Batllori et al., 2013; Ruffault et al., 2020). Process-based models have the potential to address

¹University Bordeaux, CNRS, Bordeaux INP, EPOC, UMR 5805, Pessac, France

²CEFREM UMR5110 CNRS, Université de Perpignan Via Domatia, Perpignan, France

³UMR CEFE, Université de Montpellier, CNRS, EPHE, IRD, France

⁴Aix Marseille Université, CNRS, IRD, IMBE, Aix Technopole de l'environnement Arbois Méditerranée, France

⁵University of Franche-Comté, Laboratoire Chrono-environnement, UMR 6249, France

⁶Key Laboratory of Marine Ecosystem Dynamics, Second Institute of Oceanography, Ministry of Natural Resources, Hangzhou, P. R. China

⁷LOCEAN, CNRS, Sorbonne Université, Campus Pierre et Marie Curie, France

Corresponding authors:

Marion Genet, Geo-Ocean, Université Bretagne Sud, Université Brest, CNRS, Ifremer, UMR6538, 52 Avenue Paul Alduy, 66860 Perpignan Cedex 9, Vannes F-56000, France.

Email: marion.genet17@gmail.com

Anne-Laure Daniau, University Bordeaux, CNRS, Bordeaux INP, EPOC, UMR 5805, Bat B18N, Allée Geoffroy St Hilaire, Pessac F-33600, France.

Email: anne-laure.daniau@u-bordeaux.fr

some of the feedback loops between fire, vegetation and climate but it is essential to assess the extent to which they can simulate fire under climates and human pressure that are significantly different from today (Hantson et al., 2016). Moreover, process-based models considering vegetation-fire interactions indicate that the role of vegetation productivity on fires is underestimated (Forkel et al., 2019).

To gain insight into the interplay between fire and vegetation dynamics under the range of climate and environmental conditions projected for the next centuries, it is necessary to benchmark these process-based models with paleofire records covering different climate conditions from today (Hantson et al., 2016). Furthermore, interactions between fire and its primary controls, particularly climate and vegetation, often involve lag times of years to centuries, highlighting the critical importance of long-term data on changes in the fire regime (Whitlock et al., 2010).

Charcoal records from lake and marine sediment archives capture local to regional-scale biomass burning across a wide range of historical climate states and variability (Beaufort et al., 2003; Colombaroli et al., 2007; Daniau et al., 2007; Florescu et al., 2019; Hennebelle et al., 2020; Mensing et al., 1999; Thevenon et al., 2004; Vanni  re et al., 2008) than remote sensing data (last 20 years) against which these models have mostly been benchmarked. The compilation of several hundred paleofire records, mainly from the northern hemisphere, has shown a long-term increase in global biomass burning since the Last Glacial Maximum (Daniau et al., 2012; Power et al., 2010), primarily driven by increasing temperature, with fire peaks occurring at intermediate moisture levels and aridity/productivity gradient (Daniau et al., 2012). A strong link between climate and fires has also been observed over the past 21,000 years at multi-centennial to multi-millennial timescales (Daniau et al., 2012; Marlon et al., 2016; Power et al., 2010), with notable increases in fire activity under warm conditions as long as biomass was sufficient to support fires (Krawchuk and Moritz, 2011). Marlon et al. (2016) found that climate had a pervasive impact on fire activity throughout the Holocene, across multiple spatial and temporal scales, although not ruling out the possible role of human activities at local scales and during certain time periods. Over the last century, humans were a major driver of temporal change in fire regime (Mouillot and Field, 2005) and significantly contributed to the current global fire regime spatial pattern (Bowman et al., 2011).

In the Mediterranean basin, local charcoal records reveal a complex history of fire activity during the Holocene with multiple fire controlling factors. For instance, Turner et al. (2008) observed high fire frequency in Turkey during wet periods in open and fuel-limited vegetation whereas Vanni  re et al. (2008) reported enhanced fires in Italy during dry periods in non-fuel limited forest ecosystems. Leys and Carcaillet (2016) found that fires in subalpine forests in the Swiss Alps were controlled by climate and available biomass during the early Holocene, and by social practices established around lakes during the Late-Holocene. The influence of human activities on fires has also been reported in several Mediterranean areas. For example, a human influence on fires was suggested since 5.0 ka in Corsica (Lestienne, 2019), and since 5.0 or 4.0 ka in Italy (Noti et al., 2009; Vanni  re et al., 2008). In contrast, Sweeney et al. (2022) inferred a minor human impact on fire regimes in Iberia during the early and Mid-Holocene (10,000 and 3500 cal. BP) compared to other factors such as climate and vegetation.

The paleofire history of the French Mediterranean region during the Holocene has been poorly documented while the occurrence of large summer fires in this area is nowadays a growing concern (Ruffault et al., 2017). Fires of less than 1 ha are common in this region, but the majority of the area burned is caused by rare and large fires of more than 100 ha (Ganteaume and Jappiot, 2013). Ruffault et al. (2017) identified preferential large-scale atmospheric patterns leading to large fires, defined here as those

exceeding 120 ha (corresponding to the 95th percentile of all fires included in the national wildfire inventory PROMETHEE database available from 1973 to 2013 in southeastern France). These large fires have been shown to be primarily wind-driven linked to two weather types during summer months (Ruffault et al., 2020) characterised by cold temperature, fast winds and low relative humidity, that is, a synoptic pattern similar as the Atlantic Ridge weather regime, and the negative NAO (NAO-) regime (Ruffault et al., 2017). A few large heat-driven fires occur also in the French Mediterranean region under two other weather regime types, which are the blocking like feature positive NAO regime and the Atlantic Low (Cassou et al., 2005), producing anomalously warm and dry local conditions (Ruffault et al., 2017).

This fire weather type distribution makes this dominantly wind-driven fire region particular across the Mediterranean Basin (Ruffault et al., 2020) as it departs from the common view of a dominant heat wave-driven fires in Mediterranean pyroregions. Future climate scenarios suggest a switch of fire weather frequencies from dominant wind-driven to dominant heat wave-driven fire weathers in southeastern France (Ruffault et al., 2017), questioning the contribution of the wind-driven fire weather types in the future. Yet this study relies on statistical relationships based on current fire regimes largely influenced by intensive fire suppression strategies. Fire suppression and prevention practices introduced in the 1980s in the area led to reduce large fire occurrences induced by dry/hot conditions, with fires ignited under strong wind conditions remaining hardly controlled in a sufficient amount of time before spreading to uncontrolled large fires (Ruffault and Mouillot, 2017). This bias in the statistical fire-weather relationship thus questions its reliability in being applied backward in time or for future scenarios as recently tested by Van der Meersch et al. (2025) for tree species distribution models over Europe. Combined wind and heat driven event might actually remain the most impactful fire events in the future as recently illustrated by the January 2025 California fire events (Kumar et al., 2025) that needs to be further investigated with robust datasets and models.

Here, we aim at exploring the occurrence and the drivers of large fires in southeastern France over a long time period under past diverse climate conditions, thus removing the impact of strong fire fighting policies. For this purpose, we generated a record of biomass burning in southeastern France over the past 8.2 ka, using microscopic charcoal (>10 microns in length), a proxy for fire, preserved in a marine sediment core from the Gulf of Lions. The abundance and morphology of microcharcoal were used to capture changes in fire regimes including fire frequency, fire size and the burned vegetation. We then compared our paleofire reconstruction with previous information in the region on targeted fire drivers such as human occupation, vegetation changes, oceanic and atmospheric circulation patterns in order to assess the controlling factors of fire regime variability at centennial to millennial scales and drivers of large fires in the region.

Study area, present-day climate, vegetation and fire

The French Mediterranean region includes Mediterranean lowlands, mid-elevation hinterlands and foothills and mountain areas (Figure 1; Curt et al., 2016). High elevation landscapes corresponding to the Alps mountain area are characterised by low mean annual temperature (<11.5  C) and high mean annual precipitation (>1150 mm; Curt et al., 2016), and by the ‘Temperate Conifer Forests’ biome (Olson, 2002; Figure 1). In these high altitudes, a cool and moist ecosystem dominates with the presence of *Pinus sylvestris* L., *Pinus nigra* Arn., *Fagus sylvatica* L. and *Abies alba* Mill (Curt et al., 2016) which experienced low fire activity (Hou  rou and No  l, 1987) compared to the supra-Mediterranean and montane ecosystems found at medium elevation of the Southern Alps

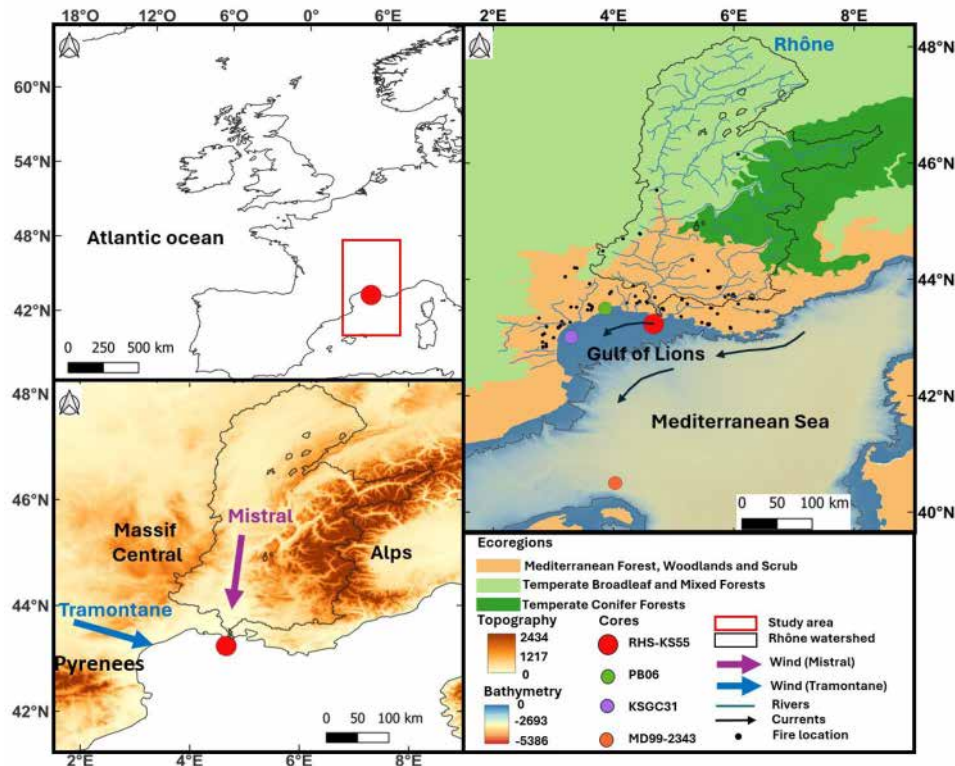


Figure 1. Study area and environmental context. Rhône watershed (Black). Rhône River (Blue). Red dot: RHS-KS55 core. Purple dot: KSGC31 core (Jalali et al., 2016). Green dot: PB06 core (Azuara et al., 2015a). Orange dot: MD99-2343 core (Frigola et al., 2007). Surface oceanic currents (black arrow). Wind direction (mistral: purple arrow, tramontane: blue arrow). Black dots: location of fires between 2001 and 2016 (FRY database (Laurent et al., 2018)). Ecoregions (Mediterranean forest, Woodlands and Scrub (light orange), Temperate Broadleaf and Mixed Forests (light green), Temperate Conifer Forests (dark green); Olson, 2002).

composed of *Larix decidua*, *Picea abies* and *Pinus cembra* (Fréjaville and Curt, 2015). These mid elevation areas are characterised by intermediate annual air temperature (11.5°C–13°C) and moderate rainfall (700–1150 mm; Curt et al., 2016) and by the ‘Temperate Broadleaf & Mixed Forests’ biome (Olson, 2002). Mediterranean lowlands are characterised by annual air temperatures > 13°C and rainfall amount < 700 mm (Curt et al., 2016) and by the ‘Mediterranean Forests, Woodlands & Scrub’ biome (Olson, 2002). Current fires in southeastern France are mainly restricted to coastal and mid-altitude (300–500 m) Mediterranean areas. Only a few of them occur in mountains (Southern Massif Central and Southern Alps; Curt et al., 2016; Fréjaville and Curt, 2015; Figure 1). In mid to low elevation areas, the vegetation is dominated by Mediterranean forests composed of sclerophyllous and evergreen trees. This vegetation is composed of flammable shrublands (so-called scrublands and maquis) including *Quercus coccifera* L., *Ulex parviflorus* Pourr., *Cistus* spp. and *Erica arborea* L. (Curt et al., 2016), most of which are active pyrophytes (Houérou and Noël, 1987) with fire-tolerant strategies (as defined in Archibald et al., 2019).

Fires in southeastern France are caused by negligence (57.8%), intentional ignitions (19.8%), accidental ignitions (12.3%) and lightning (10.1%; Curt et al., 2016). They occur primarily during the summer months (June–August) and are more frequently wind-driven than heat wave-driven (Ruffault et al., 2017). Most large fires (> 120 ha) occur under the Atlantic Ridge and NAO-weather regimes. The NAO- regime is characterised by higher-than-normal pressures over Iceland associated with larger than normal precipitation and colder conditions in winter over France (Boé, 2013) including the Mediterranean area (Bruley et al., 2022). During NAO-years, local weather conditions in summer over southeastern France are characterised by cold temperatures, strong and dry surface winds and low relative humidity favouring the occurrence of large fires (Ruffault et al., 2017).

According to Cassou et al. (2005), the Atlantic Ridge weather regime shares some similarities with the East Atlantic pattern (EAP; Barnston and Livezey, 1987). The EAP also influences the Mediterranean climate and is structurally similar to the NAO with its main centre of action being displaced south-eastward (Josey et al., 2011). The negative EAP is characterised by a strong anti-cyclonic anomaly over the eastern Atlantic and a low-pressure system in the central Mediterranean Sea (Häkkinen et al., 2011), resulting in a northeasterly flow of cold and dry air coming from boreal latitude (Josey et al., 2011) blowing over southeastern France and the Gulf of Lions (Jiang et al., 2003; Sicre et al., 2016). Our study area is thus influenced by major large-scale wind regimes funnelled by large valleys, North-Northwesterly winds, the Tramontane (between the Pyrenees and the Massif Central) and the Northerly winds, called Mistral (between the Massif Central and the Alps; Figure 1), which are related to these large-scale atmospheric circulation modes of the North Atlantic modified by the orography (Jiang et al., 2003; Monaco et al., 2009). Local winds can be funnelled by fine scale topography (Dupuy et al., 2021) driving fire spread direction as observed in California (Barros et al., 2013), but prevailing large scale atmospheric events such as Santa Ana winds remain the keystone driver of wildfires (Mensing et al., 1999) and major impactful fire as the 2025 California fire season (Kumar et al., 2025).

Materials and methods

Core location, sedimentology, sampling and chronostratigraphy

The marine sediment core RHS-KS55 (43°14.350 N; 4°40.960 E, 63 m water depth, length of the core 7.38 m, <<http://igsn.org/BFBGX-86605>>) was collected in 2008 during the RHOSOS

oceanographic cruise in the Rhone prodelta on board the R/V Le Suroît. The Rhone prodelta is made of several lobes collecting the Rhone river watershed. During the early Holocene, the outlets of the Rhone retreated landward due to sea-level rise (Berné et al., 2007), then shifted in a W-E direction during the Mid- and Late-Holocene as a result of natural avulsions, and eventually in response to man-made deviations of the stream during the middle and Late-Holocene (Fanget et al., 2016; Vella et al., 2005). Due to the development of the Rhone 'Bras de Fer' and 'Grand Passon' channels at the origin of a prodeltaic lobe at the location of the core, the sediment accumulation rates during the Holocene strongly vary both spatially and vertically. A detailed sedimentological description of core RHKS-55 as well as chronological constraints, paleoenvironmental interpretations of meiofauna and seismic and stratigraphic correlations at the scale of the entire Holocene Rhone prodelta can be found in Fanget et al. (2014, 2016). These authors showed that the bottom of the core (7.38–4.50 m) is formed of alternating silty clays and silty sands, the sand beds having an erosional base interpreted as distal tempestites deposited during the early Holocene. Between 4.6 and 4.3 m, Fanget et al. (2016) described a condensed interval corresponding to the phase of maximum landward shift of the Rhone outlet(s), when accumulation rate at the coring site was lower and winnowing occurred. Above 4.3 m, they observed an increase of the accumulation rate in relation with initiation of delta progradation, the Rhone outlet(s) shifting closer and closer with time. This interval between 4.3 and 0 m corresponds to typical distal prodeltaic environments (water depth >60 m), where deposition from suspended material outpaces any erosional process, even nowadays in a context of reduced sediment supply (Estournel et al., 2023, their figure 13). This interval corresponds to burrowed silty clays where erosional surfaces are absent, with the presence of hydrotrochites and scattered debris of bryozoans, *Turritella* sp. and bivalves.

The age model is based on linear interpolation assuming a constant sedimentation rate between eight published AMS ^{14}C dated levels and a core top age estimated to ca. 280 yr cal. BP (Supplemental Figure S1, Table S1, available online; Fanget et al., 2016) using the age-modelling approach from Blaauw (2010; CLAM package 2.4.0; implemented in R version 4.1.2; Rstudio, 2021.09.1). It was updated using the Calib8.2 radiocarbon calibration programme and the Marine20 calibration curve (Heaton et al., 2020) with a local marine reservoir age DeltaR of -140 ± 65 years calculated as an average of the nearest 10 local reservoir errors (Supplemental Table S2, available online; Fanget et al., 2016; Stuiver and Reimer, 1993; <http://calib.org>, accessed 2021-3-16). Similar age model is obtained when using age-depth modelling with Bayesian methods (Bacon software; average difference of 50 years between the two age models; and uncertainties between 200 and 500 years for both models). The upper 4.5 m of RHS-KS55 core covers the last 8.2 ka. The section between 4.5 m (8.2 ka) and 4.2 m (4.5 ka) is characterised by a very low sedimentation rate of 0.01 cm.yr^{-1} , while the sedimentation rate between 4.2 m (4.5 ka) and 0 m (0.2 ka) is characterised by a much higher sedimentation rate of 0.09 cm.yr^{-1} .

Semi-quantitative analyses of minor and major trace elements were investigated using non-destructive method on an Avaatech XRF core scanner at IFREMER (Brest, France) by scanning split sediment cores (Richter et al., 2006). Measurements were performed every 1 cm with a counting time of 20 s and a 10 and 30 kV acceleration intensity. We used the K/Ti ratio to evaluate continental soil weathering through illite input in the marine realm following the same approach as developed in the nearby core KSGC31 (Figure 1) by Bassetti et al. (2016) assuming that a high K/Ti ratio correspond to low soil weathering and conversely a low K/Ti ratio to high soil weathering in the Rhône watershed.

Contiguous microcharcoal analysis (every 1 cm) was not possible due to laboratory and time constraints, although this approach is recommended to avoid missing fire episodes. We therefore adopted a sampling scheme that minimises the number of samples to be analysed allowing the analyses of fire regimes over periods longer than a few decades and explore their controls. Core RHS-KS55 was sampled every 10 cm (sediment sample of 1 cm thick) down to 3 m (average temporal resolution of 30 years), and every 1 cm between 3 and 4.5 m (average temporal resolution of 50 years) given a median resolution of 45 years. The lower part of the core (4.5–7.38 m), corresponding to the Greenlandian, was not analysed due to the presence of sediments deposited by storms and heavily reworked (Fanget et al., 2016).

Transport and origin of microcharcoal in marine sediments

Aeolian and fluvial processes are the main transport pathways of charcoal from combustion sources to sedimentation sites (Whitlock and Larsen, 2001). Recent modelling studies suggest that microscopic charcoal up to $125 \mu\text{m}$ is deposited within a few tens to a few hundred kilometres when airborne transported from the fire site (Haliuc et al., 2023; Vachula and Rehn, 2023). Charcoals deposited in water bodies float and sink as they soak in water, with a sinking rate that depends on their size and porosity (Nichols et al., 2000). Small particles can sink in a few hours, while large particles can float for a few months to years before becoming waterlogged. In the ocean realm, charcoal can adhere to particles such as faecal pellets and filamentous aggregates, and settle by gravity to the ocean floor, similar to pollen (Dupont, 1999; Hooghiemstra et al., 2006). Given that ocean currents have little effect on pollen distribution, we expect a similar impact on microcharcoal (Dupont and Wyputta, 2003). The remobilisation of fine particles within bottom nepheloid layers provides a transport mechanism for sediments and fine particles to the deep-sea (Jouanneau et al., 1998). At the scale on the Iberian Peninsula, Genet et al. (2021) found no clear relationship between microcharcoal concentrations and the distance from the coast or water depth.

In southeastern France, fires occur mainly in lowland Mediterranean areas (Fréjaville and Curt, 2015; Figure 1) but also in middle and high altitudes in the Alps (Fréjaville et al., 2016). In our study, the microcharcoal found in the RHS-KS55 core, reaching up to $125 \mu\text{m}$ in length, can be transported by prevailing winds, such as the Mistral and Tramontane, blowing from the north-northwest to the south-southeast. On a more local scale, the charcoal particles produced within the watershed can be carried away by more localised winds, particularly in mountain valleys, and then by river runoff. The Rhône River and its tributaries as well as small coastal rivers are other major transport pathways. Therefore, we can reasonably assume that microcharcoals in our sediment core reflect fires that occurred in the Mediterranean belt and in the Rhone watershed and its tributaries. Consequently, RHS-KS55 core likely provides a reliable record to explore the variability of fire activity of southeastern France over the past 8200 ka, at multi-decadal to centennial time scales.

Microcharcoal concentration and analysis

Charcoal is formed by the incomplete combustion of the vegetation between 200°C and 600°C (Conedera et al., 2009). Following the protocol published by Daniau et al. (2009, 2013), the 180 samples (each of about 0.2 g of dry bulk sediments) were treated using 5 ml of hydrochloric acid at 37% (HCl) and 5 ml of nitric acid of 37% (HNO_3) and heated in a water bath at 70°C for an hour. Then, 10 ml of 33% hydrogen peroxide (H_2O_2) were added in the warmed solution and shaken gently for 8 h. These chemical treatments were

used to remove carbonates and organic matter. After centrifugation at 3000rpm for 7min and the removal of chemicals in excess (HCl , HNO_3 and H_2O_2), 25ml of 70% hydrofluoric acid (HF) was added to eliminate siliceous material. Finally, HCl was used to remove colloidal SiO_2 and silicofluorides formed during the HF digestion. A 1/10 dilution (using distilled water) was applied to the residue and the suspension was then filtered using a $0.45\mu\text{m}$ porosity and 47mm diameter filter. A portion of the filter was mounted on PPMA slides with ethyl acetate. The slides were polished with a PRESI polisher (The CUBE) on a flocked cloth disk for 4min. Microcharcoal analyses were carried out using an automated Leica DM6000M microscope. Only microcharcoal particles $>10\mu\text{m}$ in length that appear black in transmitted light were analysed. Microcharcoal particles up to $125\mu\text{m}$ in length were found in core RHS-KS55. Knowing the total number and the total surface area of charcoal particles in 200 view-fields, the surface scanned by the microscope (12.279mm^2), the surface area of the filter (1385.44mm^2), the weight of dry bulk sediment and the dilution factor ($D=0.1$), we calculated the microcharcoal concentration (1) in number of particles per gram of sediment (CC_{nb} in $\#.\text{g}^{-1}$) and, (2) expressed using the sum of all surface areas of microcharcoal in one sample per gram of sediment (CC_{surf} in $\text{mm}^2.\text{g}^{-1}$). Potential fragmentation of charcoal due to taphonomic processes (Leys et al., 2013) or chemical treatment (Tsakiridou et al., 2021) can lead to a biased interpretation of CC_{nb} , that is, a peak of CC_{nb} may appear in the record while the CC_{surf} remains constant. We therefore compared CC_{nb} with CC_{surf} to verify that CC_{nb} can be used to accurately describe changes in biomass burning. The shape of microcharcoal was also analysed using the elongation ratio (the length to width ratio (L/W)) of the individual microcharcoal particles. The charcoal accumulation rate, corresponding to an influx (CHAR, number of particles $\text{cm}^{-2}.\text{yr}^{-1}$) was calculated using the sedimentation rate and the dry bulk density of the sediment.

Analyses of fire regime characteristics

The Charanalysis software version 0.9 (Higuera, 2009; <http://code.google.com/p/charanalysis/>; last accessed 12/12/2022) was used to decompose the charcoal accumulation rate record (CHAR) into a CHAR-background and a CHAR-peak signals. The CHAR-background represents variations in the overall charcoal production, sedimentation, mixing and sampling process. The CHAR-peak helps identifying fire episodes, corresponding to periods with one or more fires within the sampling resolution of the sediment. The microcharcoal concentration record was linearly resampled using a constant time interval of 45 years (corresponding to the median resolution of the record) to justify the techniques used for peak analysis. This approach preserves the original structure of the charcoal data, as the resampling technique makes fewer assumptions about the charcoal deposition pattern within sampling intervals (Leys and Carcaillet, 2016). We used the moving window method smoother with a time window of 800 years. This time window was chosen to maximise the signal-noise index, given a $\text{SNI}>3$ appropriate for being confident in the fire episodes reconstructed (Kelly et al., 2011, median of $\text{SNI}=3.85$; Supplemental Figure S2, available online) and provides a good fit between the empirical and modelled CHAR-noise distributions ($\text{CHAR-peak}=\text{CHAR-noise}+\text{CHAR-fire}$; Higuera, 2009). Fire episodes were considered when the CHAR-peaks exceeded the 95th percentile of the modelled CHAR-noise distribution. Fire episodes per 1000 years were smoothed using a LOWESS to characterise long-term fire frequency (Figures 2 and 3). We then used CHAR and the CHAR-background to reconstruct the biomass burned. Breakpoint analysis was performed with Rstudio Version 1.3.1093 using package Strucchange to define statistically significant changes in fire frequency variations

and on CHAR and log-transformed CHAR to define statistical changes in charcoal accumulation.

Calibration experiments of charcoal in lake sediments (Adolf et al., 2018; Aleman et al., 2013; Duffin et al., 2008) and in marine sediments off Iberia (Genet et al., 2021) and off Africa (Haliuc et al., 2023) together with experimental studies of plant burning (Crawford and Belcher, 2014; Feurdean, 2021; Umbanhowar and Mcgrath, 1998; Vachula et al., 2021) show that graminoid burning (including grass and grass-like plants) produces microcharcoal particles with a higher elongation ratio than arboreal vegetation. The mean elongation of microcharcoal particles, which is the average of the elongated values of the microcharcoal particles for each sample in marine sediments off the Iberian Peninsula ranges from 1.43 to 2.96, with lower values reflecting tree combustion and higher values reflecting the burning of more open vegetation (Genet et al., 2021). Haliuc et al. (2023) reported a mean elongation value of <1.8 for the tree burning and >2.1 for the burning of graminoid-mixed vegetation in marine sediments off Africa. These values are lower compared to the ones reported from experiments (Vachula et al., 2021), probably linked to a mean charcoal assemblage composed of different burnt vegetation types and species in marine sediments, versus a single burned type of vegetation during experiments (Haliuc et al., 2023). In addition, Feurdean's (2021) experiments conducted on Siberian taiga vegetation shows that hot crown fires in live trees and wood, or surface hot fires in live and dead shrub leaves and wood vegetation yield a high production of squared microcharcoal. Surface cool fires in graminoids produce less charcoal and more elongated microcharcoal. Therefore, we used the mean elongation ratio, and the microcharcoal accumulation to assess major burnt vegetation types, specifically graminoid versus tree burning and fire regime type (crown or surface fires).

Additionally, microcharcoal analyses in marine surface sediment samples collected off the Iberian Peninsula showed that a high microcharcoal concentration with elongated particles indicates large fires of high intensity in open Mediterranean woodlands, whereas a low microcharcoal concentration of more squared particles is associated with small fires of low intensity in closed temperate forest (Genet et al., 2021). Based on this result, we performed a K-means clustering analysis using microcharcoal concentration and mean elongation ratio values (Figure 2a and b) using Rstudio Version 1.3.1093 and the FactoMineR (Lê et al., 2008) and Factoextra (Kassambara and Mundt, 2020) packages. According to the optimal number of clusters analysis using the Within-Cluster Sum of Squares method (Supplemental Figure S3a, available online), three fire size groups were identified: large fires (high microcharcoal concentration and elongated particles, cluster 1); small fires (low microcharcoal concentration and more squared particles, cluster -1) and intermediate-sized fires (low microcharcoal concentrations and elongated particles or high microcharcoal concentration and squared particles, cluster 0; Supplemental Figure S3b, available online). Since the data generated by clustering analysis is highly variable over time, a weighted average regression using a window width of five datapoints was applied to identify periods of large fires or increasing large fires (Supplemental Figure S3c, available online and Figure 2c).

Human activities, regional vegetation and climate indicators

Because the pollen data are not available in core KS55, we used those of the nearby core (PB06 core from the Palavas lagoon, located less than 100 km from our core site (Figure 1) to assess the relationship between fire, human activity and vegetation (Azuara et al., 2015, 2018). Pollen data from the eight closest sites in the Pollen-based reconstructions in Europe over the Holocene dataset were also used (REVEALS models Regional Estimates of

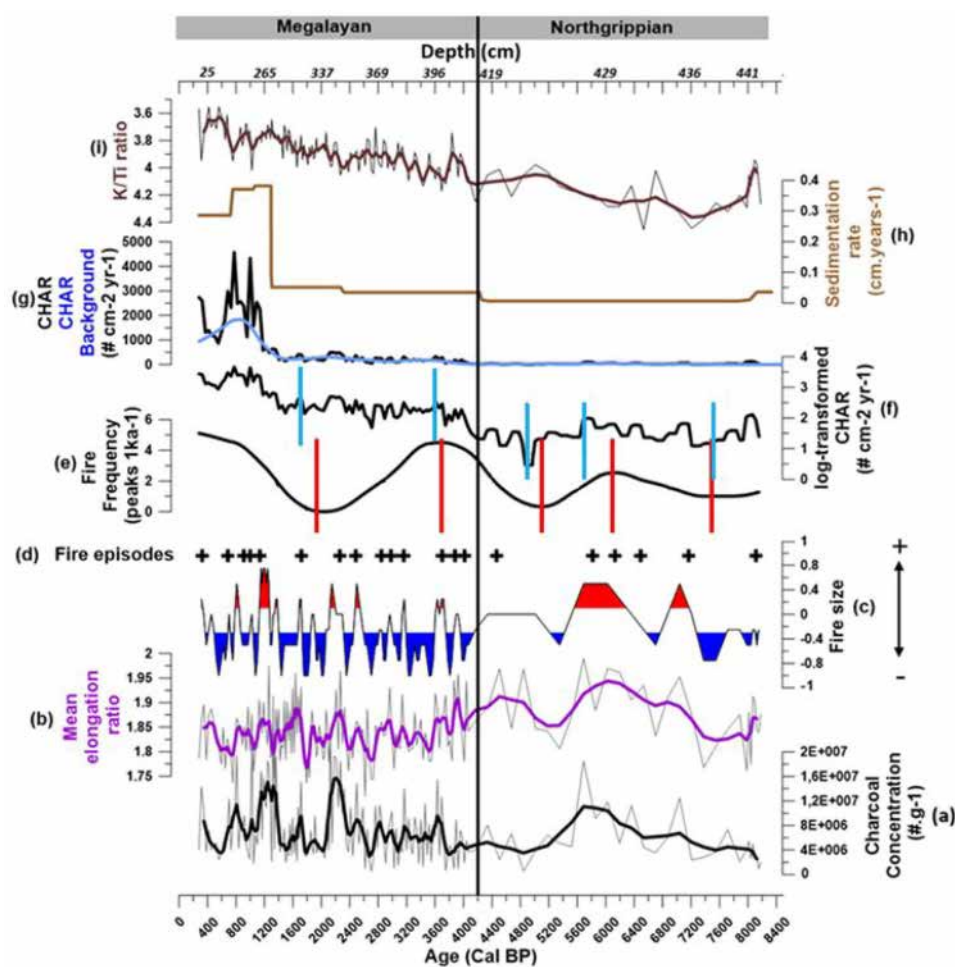


Figure 2. Microcharcoal analysis in core RSHKS55: (a) Microcharcoal concentration ($\# \text{g}^{-1}$; grey curve). A weighted average regression using a window width of five datapoints was applied (black curve). (b) Mean microcharcoal elongation ratio (grey). A weighted average regression using a window width of five datapoints was applied (purple curve). (c) Results of the cluster analysis using microcharcoal concentration and mean microcharcoal elongation ratio. A weighted average regression using a window width of five datapoints was applied (period of large fires in red and periods of small fires in blue). (d) Fire episodes, (e) Fire frequency (peaks 1ka^{-1}). (f) log-transformed CHAR ($\# \text{cm}^{-2} \text{yr}^{-1}$). (g) CHAR (black curve), CHAR background (blue curve) ($\# \text{cm}^{-2} \text{yr}^{-1}$), (h) sedimentation rate ($\text{cm} \cdot \text{yr}^{-1}$), (i) K/Ti ratio. Dotted red bars correspond to breakpoints analysis of fire frequency, dotted blue bars correspond to breakpoints analysis of log-transformed CHAR. Dotted black bar places the transition between the Northgrippian (8236–4250 ka) and the Meghalayan (4250–0 ka) stages according to Walker et al. (2019).

Vegetation Abundance from Large Sites; Githumbi et al., 2022). The relationship between fire history and human impact was evaluated based on several cultivated vegetation taxa (*Castanea*, *Cerealia*, *Poaceae*, *Juglans*, *Vitis*) from pollen analyses (Azuara et al., 2015; Githumbi et al., 2022; Figure 3c). Additionally, we used the literature review of human settlements and activities alongside the summed probability distributions of radiocarbon dates (SPD) from southern France of Berger et al. (2019) providing information on fluctuations in human population levels.

To assess changes in vegetation as a potential driver of fire regime, we used the pollen reconstruction from PB06 core (Azuara et al., 2015, 2018) and estimated the regional vegetation cover of the area using the database of Githumbi et al. (2022). The database contains plant and pollen-morphological taxa types, plant functional types (PFT) and land cover types (LCT) grouped in Evergreen trees (ET), Summer-green trees (ST) and Open land (OL; Supplemental Tables S4 and S5, available online). The percentages of LCTs of the eight nearby sites located in the southeast of France (Supplemental Figure S5, available online) were extracted for each time window (TW) over the past 8500 years (Supplemental Table S4, available online). They were then averaged for each time window and assigned to the centre of the time window (Supplemental Table S4, available online). We compared our fire regime reconstruction with dominant vegetation over the

past 8 ky, that is, mountainous, Mediterranean shrubs and herbaceous and mesophyllous taxa (Figure 4).

We also compared our fire reconstruction with paleo-records of climate variability. Several wet (5.7–5.2, 4.2–2.7, 2.4–1.8 and 1.2–0.9 ka; green rectangle in Figure 4) and dry (5.2–4.2, 2.7–2.4, 1.8–1.2 and 0.9–0.2 ka; orange rectangle in Figure 4) periods were identified over the past 6 ka based on the n-alkane Average Chain Length (ACL) from KSGC31 core in Gulf of Lions and the Log *Fagus*/Dec.*Quercus* ratio from Palavasian lagoon sediments (Figure 4f; Azuara et al., 2015; Jalali et al., 2017). We also identified summer drought episodes using the log *Fagus*/dec. *Quercus* taxa ratios from the same pollen dataset, assuming that *Fagus* is sensitive and intolerant to summer droughts (Azuara et al., 2018; Jump et al., 2006; Piovesan et al., 2008). Despite potential influences from human activity, the lack of correlation between the *Fagus* signal and anthropogenic vegetation changes (Azuara et al., 2015) and the spectral content of this time series similar to other paleoclimatic proxies (Azuara et al., 2020) supports the argument for *Fagus* being a reliable climate indicator. Therefore, low values of the log *Fagus*/Dec.*Quercus* ratio (Figure 4f) were used to identify summer drought periods at 4.8–4.2, 2.9–2.0 and 1.4–0.3 ka (pink bands in Figure 4). Note that they slightly differ from the time intervals of the dry periods obtained by Jalali et al. (2017; orange rectangle in Figure 4). Two minima

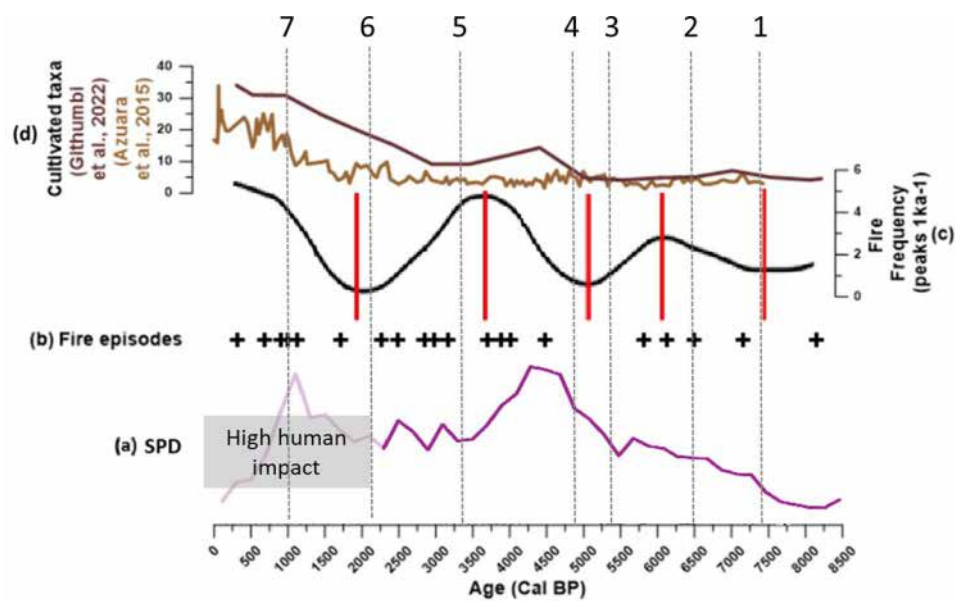


Figure 3. Comparison between fires and human activity. (a) Summed probability distribution (SPD) of unnormalised calibrated radiocarbon dates from the southern France region as a whole (Berger et al., 2019). (b) Fire episodes, (c) Fire frequency (peaks 1 ka^{-1}) in core RHS-KS55. (d) Cultivated taxa composed of *Castanea*, *Cerealia*, *Poaceae* (Githumbi et al., 2022) (dark brown curve) and *Castanea*, *Juglans*, *Vitis*, *Cerealia* type, *Poaceae* (light brown curve) (Azura et al., 2015). The dotted red bars represent the breakpoints obtained from the fire frequency curve thus delimiting periods of low and high fire frequency. The periods of human activity or migration (Berger et al., 2019) are materialised by the hatched bands captioned under the graphs. From 2.4 ka onwards, the SPD is no longer a satisfactory demographic proxy. Evidence of a high human impact is given by the high number of archaeological sites (Berger et al., 2019). Black dashed lines indicate the socio-environmental reading of the data in terms of successive thresholds: 1. Early Neolithic; 2. Chassean; 3. Chassean/Final Neolithic; 4. Early Bronze Age; 5. Final Bronze Age; 6. Classical Antiquity; 7. 1000 cal. yr BP and later (Berger et al., 2019).

in the log *Fagus*/Dec. *Quercus* ratio are also present in the older part of the record. However, we did not consider those periods as reflecting summer drought periods due to the too low percentage of *Fagus*. Furthermore, we used mean annual precipitation reconstruction of the site Embouchac located less than 100 km from our site (Herzschuh et al., 2023; Figure 4g). In order to assess potential influence of temperature on fire regimes, we compared our fire record with cold relapses identified by Jalali et al. (2016) based on alkenone-derived sea surface temperatures (SSTs; Figure 4h) reconstructed from core KSGC-31 in the Gulf of Lion (Figure 4 light blue rectangle, Supplemental Table S6, available online; 6.6–5.7, 5.3–5, 4.3–3.9, 2.5–2.1, 1.7–0.9 and 0.5–0.1 ka) and the Minorca events identified by Frigola et al. (2007; Figure 4 dark blue rectangle Supplemental Table S6, available online) based on the presence of coarse grains in deep-sea sediments north of Minorca Island (core MD99-2343 in Figure 1; 9–7.8, 7.4–6.9, 6.5–5.8, 5.3–4.7, 4.4–4, 3.4–3.1, 2.6–2.3, 1.8–1.4 and 0.8–0.2 ka).

Results

From microcharcoal record to fire regime in southeastern France

As a generic information, we estimated that microcharcoal concentrations in number of fragments per gram of sediment (CCnb in $\# \cdot \text{g}^{-1}$) vary between 5.45×10^5 and 2.91×10^7 ($\# \cdot \text{g}^{-1}$; Figure 2a), and in surface per gram of sediment (CCsurf in $\text{mm}^2 \cdot \text{g}^{-1}$) between 9.84 and 4.24×10^5 (not shown). The mean microcharcoal elongation ratios range from 1.71 to 1.99 (Figure 2b) with significantly higher values during the Northgrippian (mean elongation ratio of 1.88) than during the Meghalayan (1.84; t -test, $p < 0.05$).

We found that CCnb and CCsurf were significantly and positively correlated (Supplemental Figure S2, available online, $r = 0.95$, $p < 0.0001$; Supplemental Figure S5, available online),

from which we infer that fragmentation was minimal and that CCnb can be used as a reliable proxy of fire activity in our core. Runoff and notable erosion in the first few months after fires has been observed in French Mediterranean forest (Fox et al., 2006) and the scrublands of northwestern Spain (Soto and Diaz-Fierros, 1998). Variation in Ti and other mineral elements have been used to detect changes in fire frequency in subalpine forest (Leys et al., 2016). However, this method implies a high-resolution analysis of less than 10 years to be reliable (Pompeani et al., 2020). The absence of correlation between CCnb and the K/Ti ratio ($r = -0.087$, p -value = 0.25; Supplemental Figure S6, available online), implies that microcharcoal concentration variability in our core is not driven by weathering process, that is, charcoal washed away after deposition during Rhone river flooding. This result reinforces our assumption that charcoal concentrations do reflect changes in fire activity and not post-deposition processes, a key prerequisite to interpret our record as a paleofire record.

Regarding temporal trends, our results show that from 8.2 ka onwards, the charcoal accumulation rates (CHAR; Figure 2g) and log-transformed CHAR values (Figure 2f) have generally increased (Figure 2g), indicating a positive trend in biomass burning, and thus, that Northgrippian stage sediments have overall lower CHAR compared to the Meghalayan stage (t -test, < 0.05). Major shifts were identified in the log-transformed CHAR by breakpoint analyses centred at 7.5, 5.7, 4.9, 3.6 and 1.7 ka (Figure 2f blue vertical lines), as well as shifts in fire frequency (Figure 2f red vertical lines) centred at 7.3, 6.0, 5.1, 4.7, 3.7, 1.9 and 0.9 ka. We observed simultaneous periods of increase and decrease in log-transformed CHAR and fire frequency throughout the record, except between 3.7 and 1.9 ka, where the slight upward trend of log-transformed CHAR coincides with a decrease in fire frequency. Our fire reconstruction analysis reveals 20 fire episodes (one or multiple fires in a peak) over the past 8.2 ka (Figure 2d). This figure can be regarded as rather small considering the frequent occurrence of fires in the southeastern French region in present day. However, it should be

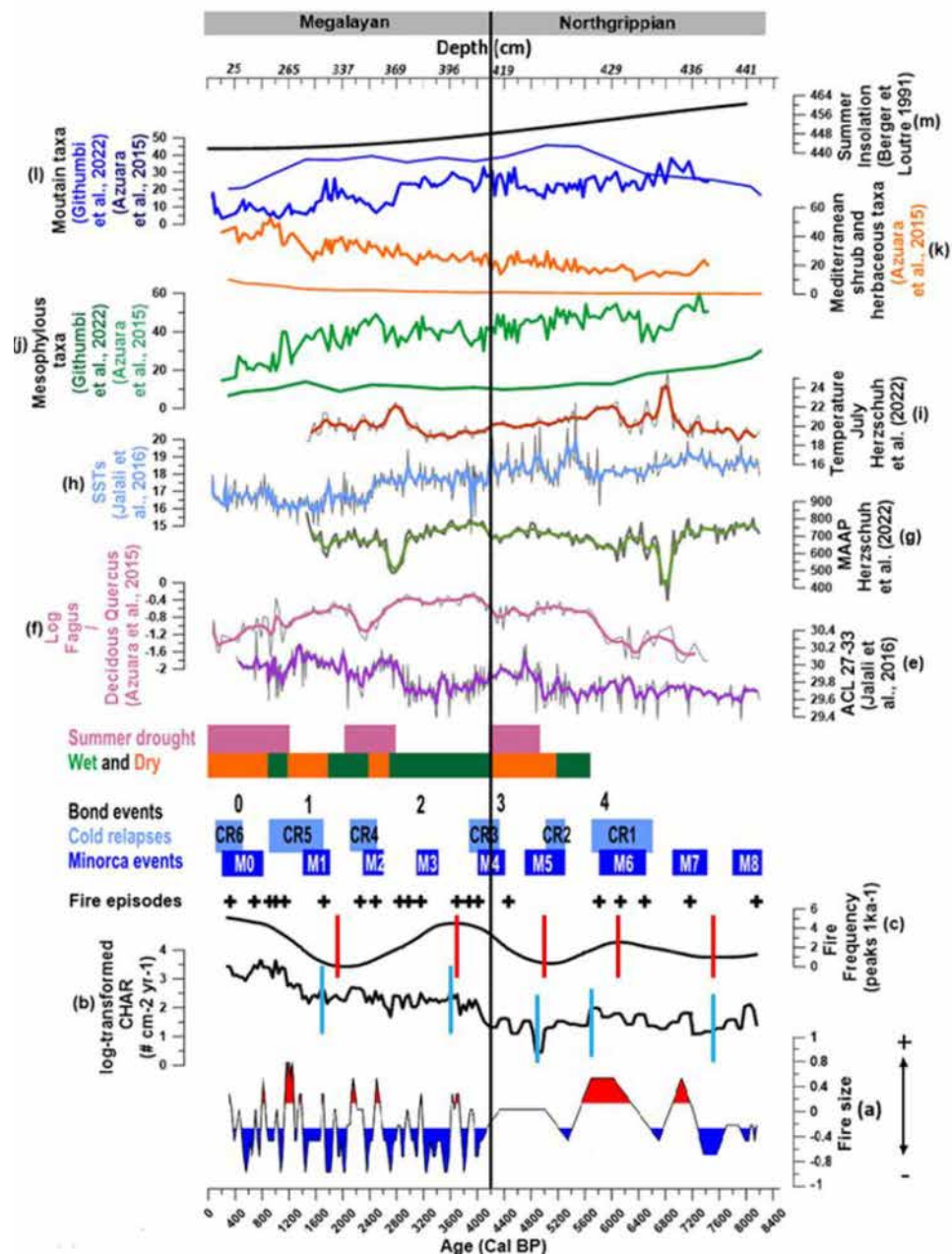


Figure 4. (a) Changes in fire size resulting from the cluster analysis using microcharcoal concentration and mean microcharcoal elongation ratio. (b) log-transformed CHAR ($\# \text{ cm}^{-2} \text{ yr}^{-1}$). (c) Fire frequency (peaks 1 ka^{-1}). (d) Fire episodes. (e) n-alkane average chain length (ACL) from KSGC31 core in Gulf of Lion (Jalali et al., 2016). (f) log *Fagus*/dec. *Quercus* ratio from Palavasian lagoon sediments (Azuara et al., 2015). (g) Mean annual precipitation in the Embouchac site (Herzschuh et al., 2023). (h) Alkenone-derived sea surface temperatures (SSTs) in the Gulf of Lions (Jalali et al., 2016). (i) July temperature in the Embouchac site (Herzschuh et al., 2023). (j–l) Relative pollen percentages from the Palavasian lagoon (Azuara et al., 2015) and percentage of estimated land cover from the regional area (Githumbi et al., 2022). Ecological groups are from Azuara et al. (2015): Mesophyllous taxa (j) include *Deciduous Quercus*, Other deciduous trees (*Acer*, *Ulmus*, *Tilia*, *Betula*, *Carpinus*, *Corylus*, *Hedera*, *Ligustrum*, *Ilex* et *Viburnum*). Mediterranean shrub and herbaceous taxa (k) include *Evergreen Quercus*, *Ericaceae*, *Evergreen shrub*, *Olea*, *Plantago*, *Rumex*, *Artemisia*. Other herbaceous taxa (*Pistacia*, *Phillyrea*, *Rhamnus*, *Buxus*, *Cistus* et *Cupressaceae*) and *Amaranthaceae*. Mountain taxa (l) include *Abies*, Other coniferous (*Picea*, *Cedrus*) and *Fagus*. Pollen taxa observed in pollen records from the region (Githumbi et al. (2022) were classified according to Azuara et al. (2015) classification. Some taxa in Azuara et al., 2015) were not present in the pollen records used by Githumbi et al. (2022). The groups formed using Githumbi et al. (2022) data differ slightly due to the absence of *Picea*, *Cedrus*, *Acer*, *Hedera*, *Ligustrum*, *Ilex*, *Viburnum*, *Rhamnus*, *Cistus*, *Cupressaceae*, *Juglan*, *Vitis* (Supplemental Table S3, available online). (m) Summer insolation (Berger and Loutre, 1991). Dotted red bars correspond to breakpoints analysis of fire frequency, dotted blue bars correspond to breakpoints analysis of log-transformed CHAR. Dotted black bars is the separation between Northgrippian and Megalayan stage according to Walker et al. (2019). A weighted average regression using a window width of 5 was applied in (e) to (h) curves.

noted that vegetation and climate conditions were not consistent throughout the past 8ka. Furthermore, it is plausible that our sampling scheme failed to capture some fire events. Using a contiguous sampling scheme Leys and Carcaillet (2016) reported 18 up to 34 fire episodes using a 700-year time window over the past 8000 years

within a subalpine ecosystem of the inner western Alps close to our site. In the west-central Pyrenees, 43 fire episodes were identified over the past 8500 years using a 250-year time window (Rius et al., 2011). Vanni  re et al. (2008) found 50 fire episodes in Italy over the past 8000 years using a 500-year time window. Consequently, the

observation of 20 fire episodes, even minimal, is certain, indicating episodes that marked the landscape sufficiently to be recorded. This appears to be a reasonable estimation when considering the length of our record, changes in the sedimentation rate and the 800-year time window of our study. Cluster analysis applied on microcharcoal concentration and mean elongation ratio led to the identification of several periods of large fires (Figure 2c).

The Northgrippian reveals a period of high fire frequency centred at 6.2 ka (Figure 2e) marked by three fire episodes (at 6.4, 6.1 and 5.8 ka; Figure 2d), and two periods of low fire frequency centred at 7.4 ka and 4.9 ka marked by three fire episodes (at 8.1, 7.1 and 4.4 ka). The Northgrippian is also punctuated by a period of large fires centred at 7.1, 5.7 and 6.0 ka. The Meghalayan is characterised by two periods of high fire frequency centred at 3.5 and 0.8 ka and marked by 10 fire episodes (4.0, 3.8, 3.7, 3.1, 2.9, 1.1, 1.0, 0.9, 0.6 and 0.3 ka) and an interval of low fire frequency centred at 2.1 ka, marked by 4 fire episodes (at 2.8, 2.4, 2.2 and 1.7 ka). This stage shows an alternation of rapid changes in the fire size with large fires at 3.7, 2.6, 2.2, 1.7, 1.3, 1.2, 0.8 and 0.4 ka (Figure 2c).

Fire and human activities

To assess the potential impact of human activities on the fire regime in the study area, we compared our fire reconstruction with a regional-scale synthesis of the dynamics of human occupation since the Neolithic. The importance of past human occupations can be seen through several proxies, including (i) the census of archaeological sites and their occupation periods (Berger et al., 2019), (ii) the collection of radiocarbon dates and their synthesis in the form of ‘summed probability distributions’ (Berger et al., 2019) and (iii) the abundance of cultivated taxa and anthropised plant formations in the pollen record (Azuara et al., 2015; Berger et al., 2019; Githumbi et al., 2022). The synthesis work of Berger et al. (2019) is particularly relevant for discussing the relationship between human activities and our fire reconstruction, as they involve similar spatial scales, covering the southeastern quarter of France.

In terms of general trends, interpretation of human occupation data suggests that population densities in southeastern France have increased monotonically since the Neolithic, generally following a logistic growth pattern, that is, rather rapidly in the early Neolithic and then more gradually from the end of this period, with several periods on shorter timescales deviating positively or negatively from this general trend (Berger et al., 2019). At the same time, there is also an upward trend in fire frequency, modulated by oscillations. These oscillations show periods of higher frequency, peaking at an ever higher level as we move towards the present. However, this rising trend shows a very different dynamic to the demographic proxies, with a more regular increase than the latter.

In the shorter term, the sequence demonstrates an interval of reduced fire frequency between 8.20 and 7.4 ka, with the occurrence of two fire episodes at 8.2 and 7.2 ka cal BP. Then begin the initial rise in fire frequency between 7.50 and 5.6 ka cal BP which corresponds to the initial phase of the Neolithic period (Cardial Neolithic) in southern France around 7.4 ka cal BP (Threshold 1, Figure 3a), followed by the Chassean period around 6.5 ka cal BP (Threshold 2, Figure 3a), a subdivision of the Neolithic in the region characterised by strong demographic dynamism and potentially a greater impact on plant landscapes linked to a development of pastoralism (Berger et al., 2019). This period saw the installation of the first agropastoral populations, the appearance and development of the first villages in the Languedoc and mid-Rhône valleys (Berger et al., 2019; Guilaine and Manen, 2005) and the first evidence of anthropogenic taxa in pollen records on a regional scale (Berger et al., 2019). The substantial development of the first agricultural populations in the area (Berger et al.,

2019) may thus have triggered an increase in fire frequency, but not to the same extent as it has been observed in some sites in the Iberian Peninsula (Carrión et al., 2010).

This is followed by a period of decreasing fire frequency between 6.0 and 5 ka (Figure 3b). The beginning of this phase corresponds to the transition between the Chassean and the Final Neolithic between 5.5 and 5.3 ka (Threshold 3, Figure 3a), this period being still culturally poorly defined (Lemerrier, 2007) and interpreted as a regional demographic recession (Berger et al., 2019). However, it appears that this demographic recession began after the onset of the decline in fire frequency, and was also much shorter.

The second period of increased fire frequency is recorded between 5 and 3.7 ka (Figure 3c). The beginning of this period corresponds to the Final Neolithic (Threshold 4, Figure 3a), between 4.8 and 4.3 ka cal BP and is interpreted as a major demographic surge throughout the region (Berger et al., 2019). This demographic pressure is evident in the first regular records of cultivated taxa in the regional pollen record (Githumbi et al., 2022). However, this demographic increase is followed by a significant period of demographic recession, one of the largest recorded by proxies in the region, between the Final Neolithic and the Early Bronze Age between 4.3 and 4.1 ka (Berger et al., 2019). Following this, there was a territorial reorganisation to the detriment of the coastal plains but in favour of the middle- and high-altitude areas until the beginning of the Final Bronze Age around 3.5 ka (Threshold 5, Figure 3a) with perhaps a slight demographic decline. Thus while fire frequency continued to increase, human pressure remained relatively low in the region.

At around 3.7 ka, the frequency of fire decreased again up to 1.8 ka, while human pressure increased again shortly after in the Final Bronze Age (3.5–3 ka), and most significantly during classical Antiquity (Threshold 6, Figure 3a), which recorded one of the highest occupation peaks of the entire sequence at around 2.2 ka cal BP (Berger et al., 2019). Finally, the last phase of increasing fire frequency begins at around 1.8 ka and continues until the present day. The onset of this phase coincides with a short period of probable demographic decline, as indicated by a decrease in the number of archaeological sites (Berger et al., 2019) and reforestation at around 1.3–1.2 ka (Azuara et al., 2015; Berger et al., 2019). Subsequently, however, the region underwent a period of significant anthropisation, characterised by a substantial population growth and dense settlement patterns across the territory (Berger et al., 2019; Threshold 7, Figure 3a). Concurrently, anthropogenic indicators, particularly cultivated taxa in pollen sequences (Castanea, Cerealia, Poaceae, Juglans and Vitis; Figure 3c), reached their peak, validating the substantial impact of human activities on the landscape (Azuara et al., 2015; Berger et al., 2019; Githumbi et al., 2022).

Fire, vegetation and climate

Apart from the influence of human activities, we further investigated the interactions between climate, vegetation and fire, by comparing our results with miscellaneous proxy of vegetation taxa and climate from previous studies (Figure 4). Since 8.2 ka, there has been a long-term increase in biomass burning (log-transformed CHAR Figure 4f) and in fire frequency (Figure 4c) associated with changes in vegetation, from a closed vegetation consisting of mesophyllous and mountain taxa (Figure 4l) to a more open vegetation composed of mediterranean shrubs and herbaceous taxa (Figure 4k). A higher number of large fires (Figure 4a) is observed when mesophyllous and mountainous vegetation dominates (Figure 4j and l), whereas smaller fires (Figure 4a) prevail when the vegetation is dominated by Mediterranean shrubs and herbaceous taxa (Figure 4k).

During the Northgrippian stage, the first decline in fire frequency (Figure 4c), biomass burning (log-transformed CHAR Figure 4b) and occurrence of small fires between 8.2 and 7.2 ka coincide with high mean annual precipitation levels exceeding 720 mm/year in the nearby Embouchac record (Figure 4g). The second decrease from 5.8 to 4.9 ka corresponds to relatively high mean annual precipitation levels and a period of wet conditions (Jalali et al., 2017). Conversely, the two increases in biomass burning (Figure 4b), high fire frequencies (Figure 4c) and large fire occurrences between 7.2 and 6 ka and between 4.8 and 4.2 ka, coincide with drier conditions in Embouchac (Figure 4i) and in the log *Fagus/Dec. Quercus* of the Palavas lagoon record (Figure 4f). Increases in biomass burning (log-transformed CHAR, Figure 4b), fires episodes (Figure 4d) and periods of large fires (Figure 4a) were mostly detected during four cold events (Figure 4, CR and M blue bands): at 8.1 ka (M8), at 7.1 ka (M7), at 6.4 ka, at 6.1 ka and at 5.8 ka (CR1/M6/Bond event) and at 4.4 and 4 ka (CR3/M4/Bond event at 4.2). Only the CR2/M5 cold event showed minimal or no fire activity (low log-transformed CHAR (Figure 4b), small fires (Figure 4a), and an extremely low frequency (Figure 4c)).

During the Meghalayan stage, biomass burning variability is small between 3.6 and 1.4 ka despite large variation in fire frequency, with high fire frequency at 4.33–2.89 ka, and low frequency at 2.89–1.45 ka. These changes of fire activity (biomass burning and fire frequency) occurred independently of moisture conditions as recorded in the log *Fagus/Dec. Quercus* and Embouchac records. However, since 1.4 ka, the notable increase in biomass burning (Figure 4b) and in fire frequency (Figure 4c) coincides with increased Mediterranean shrubs and herbaceous taxa (Figure 4k) as well as cultivated taxa (Figure 3c). During this period, 9 out of 13 fire episodes are co-eval with cold events (Figure 4 blue bands): at 3.1 ka (M3), at 2.4 and 2.2 ka (CR4/M2), at 1.7, 1.1, 1.0 and 0.9 ka (CR5/M1/Bond event at 1.4 ka), and at 0.6 and 0.3 ka (CR6/M0), a similar result as observed during the previous Northgrippian period, suggesting cold conditions as a key driver of fire activity in the region.

Discussion

Human activities influence on fires

Assessment of human impact on fire regimes is challenging, although crucial, in paleofire science (Bowman et al., 2009), and is generally inferred from the co-occurrence of a change in fire regime and indication of human presence. Increased fire frequency may indicate increased human-induced ignitions for deforestation, slash-and-burn agriculture or a shift from pasture and grazing areas to shrubland areas after land abandonment (Bowman et al., 2011). Conversely, decreased fire frequency may result from ignitions suppression, decreases in fuel amount and fuel continuity across landscapes due to practices such as pastures and grazing. During the Greenlandian (11.6–8.2 ka) in the subalpine ecosystem of the French Alps, the regional fire frequency variations were attributed to altitude, topography and slope (Carcaillet et al., 2009). Regional fire frequency was then attributed to increased human population density and activity from the Northgrippian to Meghalayan stages, linked to the reduction of woody fuel due to more intensive grazing (Carcaillet et al., 2009). The human influence on fire was evidenced during the Middle Neolithic period in the Pyrenees (Miras et al., 2007; Vanni  re et al., 2001) through the impact of sporadic agricultural practices on fire frequency between 6.0 and 5.0 ka in the west-central Pyrenees (Rius et al., 2012). In this region, fire became essential for landscape management through agro-pastoral activities after 3.0 ka (Rius et al., 2012). Vanni  re et al. (2011) reported that biomass availability and burning activity across the Mediterranean region were altered from 4000 to 3500 cal. BP onwards by land use conversion in the Bronze Age and later cultures, although this change

was particularly significant in the southern Alps (Finsinger and Tinner, 2005; Tinner and Kaltenrieder, 2005). Another large-scale study in Spain revealed that changes in land use due to agricultural practices since the Neolithic did not immediately affect fire regimes (Sweeney et al., 2022). The increase in charcoal accumulation in sediments was not directly related to the introduction of agriculture, the rapid population growth or population size, suggesting that fires were driven by additional factors such as climate (Sweeney et al., 2022).

Our charcoal record reveals changes of fire activity that do or do not coincide with human activities, thus supporting this last hypothesis. We observe periods of high fire frequency (6.80–5.59, 4.4–2.9 and 1.45–0 ka; Figure 3b) happening together with forest clearing (6.4 and 5.8 ka; Berger et al., 2019), human settlement (since 2 ka; Berger et al., 2019), or conversely, coeval with the decline of population (4.2–3.1 ka) and migration to middle and high-altitude areas (4–3.7 ka; Berger et al., 2019). We also observe fire episodes (Figure 3a) distinct from significant human activities (8.1, 7.1 and 4.4 ka) or coinciding with human activities such as the appearance of the first villages (7.7 ka), agro-pastoral activity (7.2 ka), or rapid colonisation (5.3 ka; Berger et al., 2019; Figure 3). In this case, the co-occurrence of fire episodes and human activities may be indicative of forest clearing to facilitate agriculture (Pyne, 1997). The high fire frequency observed since 1.45 ka (Figure 3b) might be linked to increase in human density since 2 ka in the area (Berger et al., 2019; Figure 3), as supported by the significant development of cultivated taxa observed in pollen records (Azura et al., 2015; Githumbi et al., 2022; Figure 3c). However, humans can hardly explain the high fire frequency period between 4.4 and 2.9 ka (Figure 3b) since this period is marked by a significant decline in population levels after the end of the Neolithic, accompanied by a redistribution of settlements on a regional scale to the detriment of lowland areas (Berger et al., 2019). The simultaneous increase in the K/Ti ratio and CHAR in our record at 4 ka may indicate a change in land use for agricultural purposes, increasing soil erosion and leading to a shift in biomass availability and fire activity. However, the K/Ti ratio increases all the way through the record, several millennia before the CHAR increase.

Lower mean elongation ratios during the Meghalayan (Figure 2b) suggests burning of trees during this period (Feurdean 2021; Genet et al., 2021; Vachula et al., 2021). Given that our marine archive records a large catchment area, it is tempting to link the human migration episode at 4–3.7 ka (Berger et al., 2019) to the hinterland with anthropogenic burning of temperate woodlands found in the area. However, a lower elongation ratio is observed not only during the migration episode (4–3.7 ka) but throughout the Meghalayan stage. Therefore, it remains tricky to assign fire activity changes after 4000 years to human activities or other prominent fire drivers such as climate (Sweeney et al., 2022) or vegetation (Keeley and Pausas, 2022) alone.

In summary, it is challenging to establish clear positive or negative correlations between the fire signal record and the history of human occupation in the study area. While it is not possible to formally rule out the influence of human activity on regional fire regimes, particularly in the Final Neolithic or from the Middle Ages onwards, the data currently available do not allow for straightforward corroboration of such a link. The most effective approach to addressing the intricate relationships between fire signals and anthropisation would be through studies of fire dynamics at smaller spatial scales.

Long-term fire regime changes during the Holocene

We explored the hypothesis that the increase of biomass burning (Figure 4b) and fire frequency (Figure 4c) since 8.2 ka is the consequence of changes in vegetation types. From the mid to Late-Holocene, decreasing summer insolation (Figure 4m) is contemporaneous

with a gradual shift in vegetation in the French Mediterranean region, transitioning from relatively closed mesophyte forests composed of mesophilous and mountain taxa, to open Mediterranean vegetation composed of Mediterranean shrubs and herbaceous taxa (Azuara et al., 2015; Githumbi et al., 2022; Figure 4k) reflecting increasing aridity throughout the Holocene. Currently, in southeastern France, open canopy forests (dry-subalpine and open-Mediterranean forests) are more susceptible to fires than closed canopy forests (moist-montane, closed-Mediterranean forests; Fréjaville et al., 2016). It is therefore likely that higher fire activity was driven by the expansion of open vegetation at the expense of closed vegetation during the Meghalayan compared to the Northgrippian. This result is contradictory to previous findings based on the compilation of 11 terrestrial records from Spain and Italy covering the meso-mediterranean region (40–45°N latitude), where biomass burning was higher during the Northgrippian than the Meghalayan (Vannière et al., 2011). Higher fire activity during the Northgrippian was attributed to woodland expansion, increased seasonality and summer drought, whereas reduced summer insolation and drought would be responsible for decreased fire activity during the Meghalayan (Vannière et al., 2011).

Our data suggest that long-term biomass burning in southeastern France likely reflects climate, vegetation and fire interactions specific to this region. During the Northgrippian, the southeastern France was dominated by closed mesophyte forest, a vegetation, composed of broadleaf trees characterised by a low flammability due to its high leaf moisture content, its low concentration of volatile compounds (such as waxes and resins), and the shade it provides by large leaves (Paritsis et al., 2015). This configuration, combined with an appropriate fire prone understory (strong flammability) composed of graminoids, creates a humid microclimate that limits the risk of ignition and the spread of fires (Rogers et al., 2020). During this period, lower amounts of microcharcoal may be attributed either to a limited microcharcoal production attributable to small fires (Adolf et al., 2018; Duffin et al., 2008) or the prevalence of surface cool fires (Feurdean, 2021). Additionally, higher elongated charcoal particles during the Northgrippian (Figure 2b) point to the burning of graminoids (Feurdean, 2021; Genet et al., 2021; Vachula et al., 2021), suggesting that fires primarily spread in the understory of closed vegetation characteristic of this period.

During the Meghalayan, open Mediterranean vegetation dominated the southeast of France (Azuara et al., 2015; Githumbi et al., 2022). This vegetation, composed of woody species, shrubs and grasses, is often highly flammable (Pausas et al., 2017). In Mediterranean forests, the vertical and horizontal continuity of fuels (Keeley, 2012), along with the presence of many small flammable trees in the understory, allows fire to spread to the canopy, thus creating crown fires (Alvarez et al., 2012). Higher amounts of microcharcoal during the Meghalayan than the Northgrippian suggest an increase in microcharcoal production due to an increased fire size (Adolf et al., 2018; Duffin et al., 2008), the prevalence of surface or crown hot fires (Feurdean, 2021) or an increase in more flammable vegetation. The presence of more squared charcoal particles during this period (Figure 2b) suggests the burning of trees (Feurdean, 2021; Genet et al., 2021; Vachula et al., 2021) or shrub leaves (Feurdean, 2021; Vachula et al., 2021). The Meghalayan being characterised mainly by an open vegetation including Mediterranean shrubs and herbaceous taxa, and by small fires, we can hypothesise that surface hot fires burning shrub leaves were dominant during this period.

Centennial and millennial-scale fire regime variability

Fire, fuel type and moisture conditions. During the Northgrippian, intervals of increased biomass burning (7.2–6.8 ka, 6.6–5.6 ka;

Figure 4b) may be due to frequent large surface cool fires (Figure 4a) burning graminoids in the understory of closed vegetation, resulting in increased production of elongated particles (Adolf et al., 2018; Genet et al., 2021). We infer that large fires reflect summer droughts as dry summers contribute to large burned areas in the Mediterranean basin today (Turco et al., 2017). Our inference is supported by the reconstruction of high mean July temperature in Embouchac record between 7.2 and 5.4 ka (Herzschuh et al., 2023). Drier climatic conditions could have promoted plant flammability and intensified fire activity (Harrison et al., 2010; Pausas and Paula, 2012) as observed in forested regions of Italy during dry conditions of the Holocene (Vannière et al., 2008). The decreases in biomass burning at 8.2–7.2, 6.8–6.6 and 5.6–4.2 ka could be explained by scarce small hot fires (Figure 4a) in closed vegetation resulting in the production of small amounts of squared microcharcoal (Adolf et al., 2018; Genet et al., 2021). Furthermore, the wet conditions in the 5.7–5.2 ka interval may have contributed to the decrease in biomass burning from 5.8 to 4.9 ka by reducing fuel flammability (Pausas and Paula, 2012). Our inference is supported by the reconstruction of high (8.2–7.2 ka) or increased (8.2–7.2 ka) mean annual precipitation in Embouchac record.

During the Meghalayan we observe a relatively high and stable biomass burning period between 3.6 and 1.4 ka marked by rapid alternations of small and large fires regardless of the wet periods at 4.2–2.7 and 2.4–1.8 ka (green rectangle in Figure 4) and dry periods at 2.7–2.4 ka. These fires may have been driven by the expansion of Mediterranean shrubs and herbaceous taxa, a flammable vegetation (Azuara et al., 2015; Githumbi et al., 2022; Figure 4k), resulting in a higher biomass burning irrespective of the climate conditions. Turner et al. (2008) documented enhanced fire activity in open vegetation during wet periods in Turkey due to fuel load increases. We therefore suggest that wet conditions during the Meghalayan were not limiting fires, as observed in Spain in the early 20th century when high human and grazing pressures were limiting fuel amount to burn thus making burned area independent of drought/wet events (Pausas and Fernández-Muñoz, 2012). After 1.4 ka, the high biomass burning rise coincided with summer drought episodes (orange rectangle in Figure 4) that exacerbated plant flammability and biomass burning.

Fire and cold events in the French Mediterranean region. Beside the most relevant fire/drought relationship evidenced for the Mediterranean basin, our results also suggest a relationship with cold events. Our study region experienced a progressive decrease of sea surface temperatures along with decreasing boreal summer insolation, and several superimposed cold relapses (CRs; Jalali et al., 2016) over the past 8.2 ka (blue rectangle in Figure 4). These events, including the Minorca events (M; Frigola et al., 2007; Supplemental Table S6, available online), were linked to negative NAO phases, leading to humid conditions and intensified winter winds in the northwest Mediterranean Sea. The synchronicity between Minorca events and cold relapses was not always observed possibly due to local factors or uncertainties in the age models. The absence of cooling in the continental shelf of the Gulf of Lion (KSGC31 core) during the M3, M7 and M8 could suggest that Mistral winds were either weaker or did not affect the continental shelf waters of the Gulf of Lion, while deep convection may have occurred in offshore open ocean waters (Jalali et al., 2016). Sicre et al. (2016) suggested that the EAP played a major role in the expression of cold relapses (CRs) during the Little Ice Age and the 4.2 ka event (Jalali et al., 2016). Increased biomass burning in charcoal paleo records from southeastern Spain (Carrión et al., 2004), central Italy (Vannière et al., 2008), Turkey (Turner et al., 2008) and Romania (Florescu et al., 2019) were evidenced during CR1, CR3 and CR4 and in Balearic Islands (Burjachs et al., 2017) during CR1 and CR3. Florescu et al. (2019) reported higher biomass burning during CR5 and

CR6 in mid-latitude European records of Romania. According to these authors, increased biomass burning during some CRs could reflect a relationship between wildfire activity in Europe, enhanced IRD flux in the North Atlantic and solar activity during the Holocene (Florescu et al., 2019).

Our record of fire activity shares strong resemblances with European records of biomass burning. Indeed, 16 out of the 20 fires episodes (Figure 4d) coincide with cooling conditions associated with enhanced wind on the continent (CRs and M), 5 out of 6 during the Northgrippian and 11 out of 14 during the Meghalayan. Additionally, we observe large fires associated with cooling during the Northgrippian, whereas there is no clear relationship during the Meghalayan stage. The absence of fire episodes or the scarcity of small fires during the CR2/M5 in our record could reflect wet conditions at this time as attested by the highest percentage of mountain taxa at regional scale (Githumbi et al., 2022).

Today, large fires in the French Mediterranean region are classified into two categories: those induced by heat waves and those induced by winds (Hernandez et al., 2015). Large fires (>120 ha) are less common in the heat-wave mode, associated with Blocking and 'Atlantic Low' regimes and characterised by warm anomalies, moist air and moderate winds (Ruffault et al., 2017). Large fires are 1.5 times more likely to occur during NAO- and Atlantic Ridge regimes (Ruffault et al., 2017), under cooler temperatures, strong dry winds and low humidity. Today, frequent NAO- in the Mediterranean region lead to increased winter precipitation (Hurrell, 2003) thereby contributing to higher fuel loads. Negative NAO during summer result in fast, dry surface winds and low humidity in southeastern France, increasing fuel flammability and fire size (Ruffault et al., 2017).

Overall, our microcharcoal data provide evidence that fire activity and the occurrence of large fires during the CRs (Frigola et al., 2007; Jalali et al., 2016) were mainly triggered by negative NAO synoptic atmospheric circulation pattern. We therefore suggest that wind-driven large fires are an inherent element of fire and weather patterns in this area rather than the result of fire suppression strategies leading to uncontrollable large fires. Our data also show that large fires occurring outside CRs were likely initiated by the heat-wave mode induced by Blocking or Atlantic Low patterns.

Perspectives for future fires

Paleo-fire reconstructions provide essential data to enrich our understanding of the interactions between fire, humans, vegetation and climate over different time scales. However, some limitations remain in applying fire regimes derived from past microcharcoal observations to the management of future wildfires. Indeed, our paleofire study provides rough estimations that are difficult to translate into actionable landscape management or firefighting operations. Nevertheless, this approach can provide qualitative trajectories in a warming world.

Future climate scenarios predict a shift from wind-dominated to heatwave-dominated fire regimes, questioning the future significance of wind-related fire weather types (Ruffault et al., 2020). Our results show that large fires associated with negative NAO prevailed during the Northgrippian, which is part of the Holocene Thermal Maximum (11–5 kyr BP; Kaufman and Broadman, 2023) where conditions were warmer than the pre-industrial period (Fischer et al., 2018). From this paleo-perspective, we suggest that large wind-driven fires might still occur under warmer conditions than the pre-industrial in southeastern France, adding to the predicted increase of heat-driven fires, potentially leading to extreme events as the California winter 2025 fire season combining drought anomalies and extreme Santa Ana winds (Kumar et al., 2025). Furthermore, given the projections of summer aridity increase in Europe the probability of extremely large wildfires (>2500 ha) in Mediterranean biomes is expected to rise (Grünig et al., 2023). However, our results suggest that prolonged aridity on millennial

timescale lead to a long-term increase in the frequency of small fires as open Mediterranean woodlands develop.

These results underscore the need to adapt fire management strategies to account for this evolving fire dynamic, integrating both the likelihood of large fires and the potential increase in the frequency of small fires within the framework of intervention planning and ecosystem protection and conservation.

Conclusion

Microcharcoal particles accumulated in the sediments off the Rhone River mouth evidence a long-term increase in fire activity over the past 8.2 ka from the Northgrippian to the Meghalayan. We showed that this trend is associated with a shift in vegetation from mountainous and mesophyllous forest to more open vegetation. Frequent and large fires during the Northgrippian stage likely spread in the understory of mountainous temperate vegetation composed of graminoids and appeared to have occurred primarily during cold events and summer drought conditions. Only short periods of scarce small fires from burning of trees were identified. Prevailing large fires during the Northgrippian were likely favoured by atmospheric conditions similar to negative NAO weather regime, owing to wet conditions favourable to fuel load accumulation in winter, combined with dry and cold summer winds enhancing fuel flammability. This peculiarity of a wind-driven fire region based on current fire/weather analysis, is thus confirmed by our paleoecological record as being an intrinsic fire/weather attribute rather than a consequence of the current fire/weather analysis that is biased towards more wind-driven uncontrollable large fires due to fire suppression strategies. The Meghalayan stage was dominated by generally more frequent but smaller shrub fires. No systematic relationship could be established between large fires and cold events during that period but fire episodes often coincided with CRs. Enhanced fire activity relative to the Northgrippian stage is supported by the development of open Mediterranean shrubland and herbaceous vegetation with increased aridity. We suggest that, during the Meghalayan, human activities might have amplified climate driven changes in fire activity, or change in fire prone vegetation development.

Acknowledgements

This work was supported by the French INSU (Institut National des Sciences de l'Univers) programme LEFE (Les Enveloppes Fluides et l'Environnement) CAMPFIRE project; by the ANR BRAISE project, grant ANR-19-CE01-0001-01 of the French Agence Nationale de la Recherche. M. Genet was supported by a doctoral fellowship from the University of Bordeaux. We thank Muriel Georget for laboratory assistance. We thank CNRS for MAS salary support. We thank Anne-Sophie Fanget for her technical support for XRF measurements. Bernard Dennielou, as well as the IFREMER and Genavir teams aboard Le Suroit greatly contributed to the quality of the retrieved core RHS-KS55. We are thankful to two anonymous reviewers for their comments, which helped improved this manuscript.

Author contributions

Marion Genet: Conceptualisation; Formal analysis; Investigation; Methodology; Resources; Writing – original draft.

Anne-Laure Daniau: Conceptualisation; Funding acquisition; Investigation; Methodology; Resources; Writing – original draft.

Florent Mouillot: Methodology; Writing – review & editing.

Bérangère Leys: Methodology; Writing – review & editing.

Maria-Angela Bassetti: Writing – review & editing.

Julien Azuara: Investigation; Writing – review & editing.

Bassem Jalali: Investigation; Writing – review & editing.

Marie-Alexandrine Sicre: Writing – review & editing.








Serge Berné: Resources; Writing – review & editing.

Muriel Georget: Resources.

Funding

The author(s) received no financial support for the research, authorship, and/or publication of this article.

ORCID iDs

Marion Genet  <https://orcid.org/0000-0002-9797-2601>
 Anne-Laure Daniau  <https://orcid.org/0000-0002-1621-3911>
 Bérangère Leys  <https://orcid.org/0000-0001-5485-0156>
 Maria-Angela Bassetti  <https://orcid.org/0000-0003-3092-0046>
 Bassem Jalali  <https://orcid.org/0000-0002-4171-1664>
 Marie-Alexandrine Sicre  <https://orcid.org/0000-0002-5015-1400>
 Serge Berné  <https://orcid.org/0000-0003-1332-5018>

Supplemental material

Supplemental material for this article is available online.

References

- Adolf C, Doyon F, Klimmek F et al. (2018) Validating a continental European charcoal calibration dataset. *Holocene* 28: 1642–1652.
- Aleman JC, Blarquez O, Bentaleb I et al. (2013) Tracking land-cover changes with sedimentary charcoal in the Afrotropics. *Holocene* 23(12): 1853–1862.
- Alvarez A, Gracia M, Vayreda J et al. (2012) Patterns of fuel types and crown fire potential in *Pinus halepensis* forests in the Western Mediterranean Basin. *Forest Ecology and Management* 270: 282–290.
- Archibald S, Hempson GP and Lehmann C (2019) A unified framework for plant life-history strategies shaped by fire and herbivory. *New Phytologist* 224(4): 1490–1503.
- Azuara J, Combourieu-Nebout N, Lebreton V et al. (2015) Late Holocene vegetation changes in relation with climate fluctuations and human activity in Languedoc (southern France). *Climate of the Past* 11(12): 1769–1784.
- Azuara J, Lebreton V, Peyron O et al. (2018) The Holocene history of low altitude Mediterranean *Fagus sylvatica* forests in southern France. *Journal of Vegetation Science* 29(3): 438–449.
- Azuara J, Lebreton V, Dezileau L et al. (2020) Middle and Late Holocene vegetation history of the Murcia region from a new high-resolution pollen sequence from the Mar Menor lagoon. *Journal of Archaeological Science: Reports* 31: 102353.
- Barnston AG and Livezey RE (1987) Classification, seasonality and persistence of low-frequency atmospheric circulation patterns. *Monthly Weather Review* 115(6): 1083–1126.
- Barros A, Pereira J, Moritz M et al. (2013) Spatial characterization of wildfire orientation patterns in California. *Forests* 4: 197–217.
- Bassetti M-A, Berné S, Sicre M-A et al. (2016) Holocene hydrological changes in the Rhône River (NW Mediterranean) as recorded in the marine mud belt. *Climate of the Past* 12(7): 1539–1553.
- Batllori E, Parisien M, Krawchuk MA et al. (2013) Climate change-induced shifts in fire for Mediterranean ecosystems. *Global Ecology and Biogeography* 22(10): 1118–1129.
- Beaufort L, de Garidel-Thoron T, Linsley B et al. (2003) Biomass burning and oceanic primary production estimates in the Sulu Sea area over the last 380 kyr and the East Asian monsoon dynamics. *Marine Geology* 201(1–3): 53–65.
- Berger A and Loutre MF (1991) Insolation values for the climate of the last 10 million years. *Quaternary Science Reviews* 10(4): 297–317.
- Berger J-F, Shennan S, Woodbridge J et al. (2019) Holocene land cover and population dynamics in southern France. *Holocene* 29(5): 776–798.
- Berné S, Jouet G, Bassetti MA et al. (2007) Late glacial to preboreal sea-level rise recorded by the Rhône deltaic system (NW Mediterranean). *Marine Geology* 245(1–4): 65–88.
- Blaauw M (2010) Methods and code for ‘classical’ age-modelling of radiocarbon sequences. *Quaternary Geochronology* 5(5): 512–518.
- Boé J (2013) Modulation of soil moisture–precipitation interactions over France by large scale circulation. *Climate Dynamics* 40(3–4): 875–892.
- Bond WJ, Woodward FI and Midgley GF (2005) The global distribution of ecosystems in a world without fire. *New Phytologist* 165(2): 525–538.
- Bowman DM, Balch J, Artaxo P et al. (2011) The human dimension of fire regimes on Earth. *Journal of Biogeography* 38(12): 2223–2236.
- Bowman DMJS, Balch JK, Artaxo P et al. (2009) Fire in the Earth System. *Science* 324(5926): 481–484.
- Bruley E, Mouillot F, Lauvaux T et al. (2022) Enhanced spring warming in a Mediterranean mountain by atmospheric circulation. *Scientific Reports* 12(1): 7721.
- Burjachs F, Pérez-Obiol R, Picornell-Gelabert L et al. (2017). Overview of environmental changes and human colonization in the Balearic Islands (Western Mediterranean) and their impacts on vegetation composition during the Holocene. *Journal of Archaeological Science: Reports* 12: 845–859.
- Carcaillat C, Ali AA, Blarquez O et al. (2009) Spatial variability of fire history in subalpine forests: From natural to cultural regimes. *Écoscience* 16(1): 1–12.
- Carrión JS, Fernández S, González-Sampériz P et al. (2010) Expected trends and surprises in the lateglacial and Holocene vegetation history of the Iberian Peninsula and Balearic Islands. *Review of Palaeobotany and Palynology* 162(3): 458–475.
- Carrión JS, Yll EI, Willis KJ et al. (2004) Holocene forest history of the eastern plateaux in the Segura Mountains (Murcia, southeastern Spain). *Review of Palaeobotany and Palynology* 132(3–4): 219–236.
- Cassou C, Terray L and Phillips AS (2005) Tropical Atlantic influence on European heat waves. *Journal of Climate* 18(15): 2805–2811.
- Chuvieco E, Yebra M, Martino S et al. (2023) Towards an integrated approach to wildfire risk assessment: When, where, what and how may the landscapes burn. 6(5): 5.
- Colombaroli D, Marchetto A and Tinner W (2007) Long-term interactions between Mediterranean climate, vegetation and fire regime at Lago di Massaciuccoli (Tuscany, Italy). *Journal of Ecology* 95(4): 755–770.
- Conedera M, Tinner W, Neff C et al. (2009) Reconstructing past fire regimes: Methods, applications, and relevance to fire management and conservation. *Quaternary Science Reviews* 28(5–6): 555–576.
- Crawford AJ and Belcher CM (2014) Charcoal morphometry for paleoecological analysis: The effects of fuel type and transportation on morphological parameters. *Applications in Plant Sciences* 2(8): 1400004.
- Curt T, Fréjaville T and Lahaye S (2016) Modelling the spatial patterns of ignition causes and fire regime features in southern France: Implications for fire prevention policy. 25(7): 785–796.
- Daniau A-LA-, Bartlein PJ, Harrison SP et al. (2012) Predictability of biomass burning in response to climate changes. *Global Biogeochemical Cycles* 26(4): 1–12.
- Daniau A-L, Goñi MFS and Duprat J (2009) Last glacial fire regime variability in western France inferred from microcharcoal preserved in core MD04-2845, Bay of Biscay. *Quaternary Research* 71(3): 385–396.
- Daniau A-L, Sánchez-Goñi MF, Beaufort L et al. (2007) Dansgaard-Oeschger climatic variability revealed by fire emissions in southwestern Iberia. *Quaternary Science Reviews* 26(9–10): 1369–1383.
- Daniau A-L, Sánchez Goñi MF, Martinez P et al. (2013) Orbital-scale climate forcing of grassland burning in southern Africa.

- Proceedings of the National Academy of Sciences* 110(13): 5069–5073.
- Duffin KI, Gillson L and Willis KJ (2008) Testing the sensitivity of charcoal as an indicator of fire events in savanna environments: Quantitative predictions of fire proximity, area and intensity. *Holocene* 18(2): 279–291.
- Dupont LM (1999) Pollen and Spores in Marine Sediments from the East Atlantic -A View from the Ocean into the African Continent. In: Fischer G and Wefer G (eds) *Use of Proxies in Paleoceanography*. Berlin, Heidelberg: Springer Berlin Heidelberg, pp. 523–546.
- Dupont LM and Wypulla U (2003) Reconstructing pathways of aeolian pollen transport to the marine sediments along the coastline of SW Africa. *Quaternary Science Reviews* 22(2): 157–174.
- Dupuy F, Duine G-J, Durand P et al. (2021) Valley winds at the local Scale: Correcting Routine weather Forecast using artificial neural networks. *Atmosphere* 12: 128.
- Estournel C, Mikolajczak G, Ulses C et al. (2023) Sediment dynamics in the Gulf of Lion (NW Mediterranean Sea) during two autumn–winter periods with contrasting meteorological conditions. *Progress in Oceanography* 210: 102942.
- Fanget A-S, Berné S, Jouet G et al. (2014) Impact of relative sea level and rapid climate changes on the architecture and lithofacies of the Holocene Rhone subaqueous delta (Western Mediterranean Sea). *Sedimentary Geology* 305: 35–53.
- Fanget A-S, Bassetti M-A, Fontanier C et al. (2016) Sedimentary archives of climate and sea-level changes during the Holocene in the Rhône prodelta (NW Mediterranean Sea). *Climate of the Past* 12(12): 2161–2179.
- Feurdean A (2021) Experimental production of charcoal morphologies to discriminate fuel source and fire type: An example from Siberian taiga. *Biogeosciences* 18(12): 3805–3821.
- Finsinger W and Tinner W (2005) Minimum count sums for charcoal concentration estimates in pollen slides: accuracy and potential errors. *The Holocene* 15(2): 293–297.
- Fischer H, Meissner KJ, Mix AC et al. (2018) Palaeoclimate constraints on a world with post-industrial warming of 2 degrees 2 and beyond. *Nature Geoscience* 11: 474–485.
- Florescu G, Brown KJ, Carter VA et al. (2019) Holocene rapid climate changes and ice-rafting debris events reflected in high-resolution European charcoal records. *Quaternary Science Reviews* 222: 105877.
- Forkel M, Andela N, Harrison SP et al. (2019) Emergent relationships with respect to burned area in global satellite observations and fire-enabled vegetation models. *Biogeosciences* 16(1): 57–76.
- Fox D, Berolo W, Carrega P et al. (2006) Mapping erosion risk and selecting sites for simple erosion control measures after a forest fire in Mediterranean France. *Earth Surface Processes and Landforms: The Journal of the British Geomorphological Research Group* 31(5): 606–621.
- Fréjaville T and Curt T (2015) Spatiotemporal patterns of changes in fire regime and climate: Defining the pyroclimates of south-eastern France (Mediterranean Basin). *Climatic Change* 129: 239–251.
- Fréjaville T, Curt T and Carcaillet C (2016) Tree cover and seasonal precipitation drive understorey flammability in alpine mountain forests. *Journal of Biogeography* 43(9): 1869–1880.
- Frigola J, Moreno A, Cacho I et al. (2007) Holocene climate variability in the western Mediterranean region from a deepwater sediment record. *Paleoceanography* 22(2): 1–16.
- Ganteaume A and Jappiot M (2013) What causes large fires in Southern France. *Forest Ecology and Management* 294(2): 76–85.
- Genet M, Daniau A-L, Mouillot F et al. (2021) Modern relationships between microscopic charcoal in marine sediments and fire regimes on adjacent landmasses to refine the interpretation of marine paleofire records: An Iberian case study. *Quaternary Science Reviews* 270: 107148.
- Githumbi E, Fyfe R, Gaillard M-J et al. (2022) European pollen-based REVEALS land-cover reconstructions for the Holocene: Methodology, mapping and potentials. *Earth System Science Data* 14(4): 1581–1619.
- Grünig M, Seidl R and Senf C (2023) Increasing aridity causes larger and more severe forest fires across Europe. *Global Change Biology* 29(6): 1648–1659.
- Guilaine J and Manen C (2005) From Mesolithic to early Neolithic in the western Mediterranean. In: Whittle A and Cummings V (eds) *Going Over: The Mesolithic-Neolithic Transition in the North-West Europe*. Oxford: Oxford University Press, pp.21–51.
- Häkkinen S, Rhines PB and Worthen DL (2011) Atmospheric blocking and Atlantic multidecadal ocean variability. *Science* 334(6056): 655–659.
- Haliuc A, Daniau A-L, Mouillot F et al. (2023) Microscopic charcoals in ocean sediments off Africa track past fire intensity from the continent. *Communications Earth & Environment* 4(1): 133.
- Hantson S, Arneth A, Harrison SP et al. (2016) The status and challenge of global fire modelling. *Biogeosciences* 13(11): 3359–3375.
- Harrison SP, Marlon JR and Bartlein PJ (2010) Fire in the Earth system. In: Dodson J (ed.) *Changing Climates, Earth Systems and Society. International Year of Planet Earth*. Dordrecht: Springer, pp.21–48.
- Heaton TJ, Köhler P, Butzin M et al. (2020) Marine20—The Marine Radiocarbon Age Calibration Curve (0–55,000 cal BP). *Radiocarbon* 62(4): 779–820.
- Hennebelle A, Aleman JC, Ali AA et al. (2020) The reconstruction of burned area and fire severity using charcoal from boreal lake sediments. *Holocene* 30: 1400–1409.
- Hernandez C, Drobinski P and Turquety S (2015) How much does weather control fire size and intensity in the Mediterranean region? *Annales Geophysicae* 33(7): 931–939.
- Herzschuh U, Ewald P, Schild L et al. (2023) Global REVEALS reconstruction of past vegetation cover for taxonomically harmonized pollen data sets. *PANGAEA*. DOI: 10.1594/PANGAEA.961588
- Higuera P (2009) CharAnalysis 0.9: Diagnostic and analytical tools for sediment-charcoal analysis. *User's Guide*. Montana State University, University of Illinois.
- Hooghiemstra H, Lézine A-M, Leroy SAG et al. (2006) Late Quaternary palynology in marine sediments: A synthesis of the understanding of pollen distribution patterns in the NW African setting. *Quaternary International* 148(1): 29–44.
- Houérou L and Noël H (1987) Vegetation wild fires in the mediterranean basin: Evolution and trends. *Ecologia mediterranea* 13(4): 13–24.
- Hurrell JE, Kushnir Y, Ottersen G et al. (2003) The North Atlantic Oscillation: climatic significance and environmental impact. *Geophys. Monogr* 134: 211–234.
- Jalali B, Sicre M-A, Bassetti M-A et al. (2016) Holocene climate variability in the north-western Mediterranean Sea (Gulf of Lions). *Climate of the Past* 12(1): 91–101.
- Jalali B, Sicre MA, Kallel N et al. (2017) High-resolution Holocene climate and hydrological variability from two major Mediterranean deltas (Nile and Rhone). *The Holocene* 27(8): 1158–1168.
- Jiang Q, Smith RB and Doyle J (2003) The nature of the mistral: Observations and modelling of two MAP events. *Quarterly Journal of the Royal Meteorological Society* 129(588): 857–875.
- Josey SA, Somot S and Tsimplis M (2011) Impacts of atmospheric modes of variability on Mediterranean Sea surface heat exchange. *Journal of Geophysical Research: Oceans* 116(C2).

- Jouanneau JM, Garcia C, Oliveira A et al. (1998) Dispersal and deposition of suspended sediment on the shelf off the Tagus and Sado estuaries, S.W. Portugal. *Progress in Oceanography* 42(1): 233–257.
- Jump AS, Hunt JM and Peñuelas J (2006) Rapid climate change-related growth decline at the southern range edge of *Fagus sylvatica*. *Global Change Biology* 12(11): 2163–2174.
- Kassambara A and Mundt F (2020) *Factoextra: Extract and Visualize the Results of Multivariate Data Analyses*. R Package Version 1.0.7. Available at: <https://CRAN.R-project.org/package=factoextra>
- Kaufman DS and Broadman E (2023) Revisiting the Holocene global temperature conundrum. *Nature* 614(7948): 425–435.
- Keeley JE (2012) Ecology and evolution of pine life histories. *Annals of Forest Science* 69(4): 445–453.
- Keeley JE and Pausas JG (2022) Evolutionary ecology of fire. *Annual Review of Ecology, Evolution, and Systematics* 53(1): 203–225.
- Kelly RF, Higuera PE, Barrett CM et al. (2011) Short paper: A signal-to-noise index to quantify the potential for peak detection in sediment-charcoal records. *Quaternary Research* 75(1): 11–17.
- Krawchuk MA and Moritz MA (2011) Constraints on global fire activity vary across a resource gradient. *Ecology* 92(1): 121–132.
- Kumar M, AghaKouchak A, Abatzoglou JT et al. (2025) Compounding effects of climate change and WUI expansion quadruple the likelihood of extreme-impact wildfires in California. *npj Natural Hazards* 2: 17.
- Laurent P, Mouillot F, Yue C et al. (2018) FRY, a global database of fire patch functional traits derived from space-borne burned area products. *Scientific Data* 5(1): 180132.
- Lemerrier O (2007) La Fin Du Néolithique Dans Le Sud-Est De La France. Concepts Techniques, Culturels Et Chronologiques De 1954 à 2004, In : Evin J. (Dir.) *Un Siècle De Construction Du Discours Scientifique En Préhistoire, Actes Du XXVIe Congrès Préhistorique De France*, Avignon, 21–25 September 2004, Vol. I, pp.485–500. Paris: Société Préhistorique Française.
- Lê S, Josse J and Husson F (2008) FactoMineR: An R package for multivariate analysis. *Journal of Statistical Software* 25(1): 1–18.
- Lestienne M (2019) *Quantification et modélisation de l'évolution du régime des feux au cours de l'Holocène et de l'Anthropocène en Corse*. PhD Thesis, Université Bourgogne Franche-Comté. Available at: <https://theses.hal.science/tel-02555105> (accessed 17 April 2023).
- Leys B and Carcaillet C (2016) Subalpine fires: The roles of vegetation, climate and, ultimately, land uses. *Climatic Change* 135: 683–697.
- Leys B, Carcaillet C, Dezileau L et al. (2013) A comparison of charcoal measurements for reconstruction of Mediterranean paleo-fire frequency in the mountains of Corsica. *Quaternary Research* 79(3): 337–349.
- Leys B, Higuera PE, McLauchlan KK et al. (2016) Wildfires and geochemical change in a subalpine forest over the past six millennia. *Environmental Research Letters* 11(12): 125003.
- Lohman DJ, Bickford D and Sodhi NS (2007) Environment. The burning issue. *Science* 316: 376.
- Marlon JR, Kelly R, Danialu A-L et al. (2016) Reconstructions of biomass burning from sediment-charcoal records to improve data–model comparisons. *Biogeosciences* 13(11): 3225–3244.
- Mensing SA, Michaelsen J and Byrne R (1999) A 560-year record of Santa Ana fires reconstructed from charcoal deposited in the Santa Barbara Basin, California. *Quaternary Research* 51(3): 295–305.
- Miras Y, Ejarque A, Riera S et al. (2007) Dynamique holocène de la végétation et occupation des Pyrénées andorranes depuis le Néolithique ancien, d'après l'analyse pollinique de la tourbière de Bosc dels Estanyons (2180m, Vall del Madriu, Andorre). *Comptes Rendus Palevol* 6(4): 291–300.
- Monaco A, Ludwig W, Provansal M et al. (eds) (2009) *Le golfe du Lion: Un observatoire de l'environnement en Méditerranée*. éditions Quae. Available at: <https://library.oapen.org/handle/20.500.12657/24752> (accessed 17 April 2023).
- Mouillot F and Field CB (2005) Fire history and the global carbon budget: a 1° × 1° fire history reconstruction for the 20th century. *Global Change Biology* 11(3): 398–420.
- Nichols GJ, Cripps JA, Collinson ME et al. (2000) Experiments in waterlogging and sedimentology of charcoal: Results and implications. *Palaeogeography Palaeoclimatology Palaeoecology* 164(1–4): 43–56.
- Noti R, van Leeuwen JFN, Colombaroli D et al. (2009) Mid- and late-Holocene vegetation and fire history at Biviere di Gela, a coastal lake in southern Sicily, Italy. *Vegetation History and Archaeobotany* 18(5): 371–387.
- Olson RJ (2002) *Global and regional ecosystem modeling: Databases of model drivers and validation measurements* (No. ORNL/TM-2001/196). Oak Ridge National Lab. (ORNL), Oak Ridge, TN (United States).
- Paritsis J, Veblen TT, and Holz A (2015) Positive fire feedbacks contribute to shifts from *Nothofagus pumilio* forests to fire-prone shrublands in Patagonia. *Journal of Vegetation Science* 26(1): 89–101.
- Pausas JG and Fernández-Muñoz S (2012) Fire regime changes in the western Mediterranean Basin: From fuel-limited to drought-driven fire regime. *Climatic Change* 110(1–2): 215–226.
- Pausas JG and Paula S (2012) Fuel shapes the fire–climate relationship: Evidence from Mediterranean ecosystems. *Global Ecology and Biogeography* 21(11): 1074–1082.
- Piovesan G, Biondi F, Filippo AD et al. (2008) Drought-driven growth reduction in old beech (*Fagus sylvatica* L.) forests of the central Apennines, Italy. *Global Change Biology* 14(6): 1265–1281.
- Pausas JG, Keeley JE, and Schwilk DW (2017) Flammability as an ecological and evolutionary driver. *Journal of Ecology* 105(2): 289–297.
- Pompeani DP, McLauchlan KK, Chileen BV et al. (2020) The biogeochemical consequences of late Holocene wildfires in three subalpine lakes from northern Colorado. *Quaternary Science Reviews* 236: 106293.
- Power MJ, Marlon JR, Bartlein PJ et al. (2010) Fire history and the Global Charcoal Database: A new tool for hypothesis testing and data exploration. *Palaeogeography Palaeoclimatology Palaeoecology* 291(1–2): 52–59.
- Pyne S (1997) *World fire: The culture of fire on Earth* - Stephen J. Pyne - Google Livres. Available at: https://books.google.fr/books?hl=fr&lr=&id=W0TbAwAAQBAJ&oi=fnd&pg=PR7&dq=Pyne+1995+fire&ots=5NtwqaXudk&sig=qaUu4omiU4mdYjbnj-2A9axbdc0&redir_esc=y#v=onepage&q=Pyne%201995%20fire&f=false (accessed 24 November 2023).
- Richter TO, van der Gaast S, Koster B et al. (2006) The Avaatech XRF Core Scanner: technical description and applications to NE Atlantic sediments. *Geological Society London Special Publications* 267(1): 39–50.
- Rius D, Vannièr B, Galop D et al. (2011) Holocene fire regime changes from multiple-site sedimentary charcoal analyses in the Lourdes basin (Pyrenees, France). *Quaternary Science Reviews* 30(13–14): 1696–1709.
- Rius D, Vannièr B and Galop D (2012) Holocene history of fire, vegetation and land use from the central Pyrenees (France). *Quaternary Research* 77(1): 54–64.
- Rogers BM, Balch JK, Goetz SJ et al. (2020) Focus on changing fire regimes: interactions with climate, ecosystems, and society. *Environmental Research Letters* 15(3): 030201.

- Ruffault J, Curt T, Moron V et al. (2020) Increased likelihood of heat-induced large wildfires in the Mediterranean Basin. *Scientific Reports* 10(1): 13790.
- Ruffault J, Moron V, Trigo RM et al. (2017) Daily synoptic conditions associated with large fire occurrence in Mediterranean France: Evidence for a wind-driven fire regime: Daily synoptic conditions associated with large fire occurrence. *International Journal of Climatology* 37(1): 524–533.
- Ruffault J and Mouillot F (2017) Contribution of human and biophysical factors to the spatial distribution of forest fire ignitions and large wildfires in a French Mediterranean region. *International Journal of Wildland Fire* 26(6): 498–508.
- San-Miguel-Ayanz J, Durrant T, Boca R et al. (2019) Forest fires in Europe, Middle East and North Africa 2018. Available at: <https://publications.jrc.ec.europa.eu/repository/handle/JRC117883> (accessed 17 April 2023).
- Sicre M-A, Jalali B, Martrat B et al. (2016) Sea surface temperature variability in the North Western Mediterranean Sea (Gulf of Lion) during the Common Era. *Earth and Planetary Science Letters* 456: 124–133.
- Soto B and Díaz-Fierros F (1998) Runoff and soil erosion from areas of burnt scrub: comparison of experimental results with those predicted by the WEPP model. *Catena* 31(4): 257–270.
- Stuiver M and Reimer PJ (1993) Extended 14C data base and revised CALIB 3.0 14C age calibration program. *Radiocarbon* 35(1): 215–230.
- Sweeney L, Harrison SP and Linden MV (2022) Assessing anthropogenic influence on fire history during the Holocene in the Iberian Peninsula. *Quaternary Science Reviews* 287: 107562.
- Thevenon F, Bard E, Williamson D et al. (2004) A biomass burning record from the West Equatorial Pacific over the last 360 ky: Methodological, climatic and anthropic implications. *Palaeogeography Palaeoclimatology Palaeoecology* 213(1–2): 83–99.
- Tinner W and Kaltenrieder P (2005) Rapid responses of high-mountain vegetation to early Holocene environmental changes in the Swiss Alps. *Journal of Ecology* 93(5): 936–947.
- Tsakiridou M, Cunningham L and Hardiman M (2021) Toward a standardized procedure for charcoal analysis. *Quaternary Research* 99: 329–340.
- Turco M, von Hardenberg J, AghaKouchak A et al. (2017) On the key role of droughts in the dynamics of summer fires in Mediterranean Europe. *Scientific Reports* 7(1): 81.
- Turner R, Roberts N and Jones MD (2008) Climatic pacing of Mediterranean fire histories from lake sedimentary micro-charcoal. *Global and Planetary Change* 63(4): 317–324.
- Umbanhowar CE and Mcgrath MJ (1998) Experimental production and analysis of microscopic charcoal from wood, leaves and grasses. *Holocene* 8(3): 341–346.
- Vachula RS and Rehn E (2023) Modeled dispersal patterns for wood and grass charcoal are different: Implications for paleo-fire reconstruction. *Holocene* 33: 159–166.
- Vachula RS, Sae-Lim J and Li R (2021) A critical appraisal of charcoal morphometry as a paleofire fuel type proxy. *Quaternary Science Reviews* 262: 106979.
- Van der Meersch V, Armstrong E, Mouillot F et al. (2025) Paleo-records reveal biological mechanisms crucial for reliable species range shift projections amid rapid climate change. *Ecology Letters* 28: e70080.
- Vanni  re B, Colombaroli D, Chapron E et al. (2008) Climate versus human-driven fire regimes in Mediterranean landscapes: The Holocene record of Lago dell'Accesa (Tuscany, Italy). *Quaternary Science Reviews* 27(11–12): 1181–1196.
- Vanni  re B, Galop D, Rendu C et al. (2001) Feu et pratiques agropastorales dans les Pyr  n  es-Orientales : le cas de la montagne d'Enveitg (Cerdagne, Pyr  n  es-Orientales, France). *Sud-Ouest europ  en* 11(1): 29–42.
- Vanni  re B, Power MJ, Roberts N et al. (2011) Circum-Mediterranean fire activity and climate changes during the mid-Holocene environmental transition (8500–2500 cal. BP). *Holocene* 21(1): 53–73.
- Vella C, Fleury T-J, Raccasi G et al. (2005) Evolution of the Rh  ne delta plain in the Holocene. *Marine Geology* 222–223: 235–265.
- Walker M, Head MJ, Lowe J et al. (2019) Subdividing the Holocene Series/Epoch: Formalization of stages/ages and sub-series/subepochs, and designation of GSSPs and auxiliary stratotypes. *Journal of Quaternary Science* 34(3): 173–186.
- Whitlock C and Larsen C (2001) Charcoal as a fire proxy. In: Smol JP, Birks HJB, Last WM et al. (eds) *Tracking Environmental Change Using Lake Sediments: Terrestrial, Algal, and Siliceous Indicators*. Developments in Paleoenvironmental Research. Dordrecht: Springer, pp.75–97.
- Whitlock C, Higuera PE, McWethy DB et al. (2010) Paleoeological perspectives on fire ecology: revisiting the fire-regime concept. *The Open Ecology Journal* 3(1): 6–23.